Neurobiology of Pain 18 (2025) 100181

Contents lists available at ScienceDirect

Neurobiology of Pain

journal homepage: www.sciencedirect.com/journal/neurobiology-of-pain

Voluntary exercise prevents and eradicates anxiety-like behavior by influencing parvalbumin-positive neurons, perineuronal nets, and microglia activation in corticolimbic regions of neuropathic pain rats

Thu Nguyen Dang [a,b], Cuong Nguyen Van [a], Ryosuke Ochi [a,c], Hiroki Kuwamura [a], Tomoyuki Kurose [d], Yoki Nakamura [e], Kazue Hisaoka-Nakashima [e], Norimitsu Morioka [e], Hisao Nishijo [f], Naoto Fujita [a,g], Susumu Urakawa [a,*]

[a] Department of Neurorehabilitation and Emotional Science, Graduate School of Biomedical and Health Sciences, Hiroshima University, 1-2-3 Kasumi, Minami-ku, Hiroshima City, Hiroshima 734-8553, Japan
[b] Department of Anesthesiology, Military Hospital 103, Vietnam Military Medical University, No. 261 Phung Hung Street, Ha Dong District, Hanoi 12108, Viet Nam
[c] Department of Anatomy and Neuroscience, Graduate School of Medical Sciences, Kyushu University, 3-1-1 Maidashi, Higashi-ku, Fukuoka City, Fukuoka 812-8582, Japan
[d] Department of Anatomy and Histology, Graduate School of Biomedical and Health Sciences, Hiroshima University, 1-2-3 Kasumi, Minami-ku, Hiroshima City, Hiroshima 734-8553, Japan
[e] Department of Pharmacology, Graduate School of Biomedical and Health Sciences, Hiroshima University, 1-2-3 Kasumi, Minami-ku, Hiroshima City, Hiroshima 734-8553, Japan
[f] Faculty of Human Sciences, University of East Asia, 2-12-1 Ichinomiya Gakuen-cho, Shimonoseki City, Yamaguchi 751-8503, Japan
[g] Department of Bio-Environmental Adaptation Sciences, Graduate School of Biomedical and Health Sciences, Hiroshima University, 1-2-3 Kasumi, Minami-ku, Hiroshima City, Hiroshima 734-8553, Japan

ARTICLE INFO

Keywords:
Voluntary exercise
Anxiety-like behavior
Neuropathic pain
Parvalbumin-positive neurons
Perineuronal nets
Microglia
Corticolimbic regions

ABSTRACT

Anxiety-like behavior often emerges in the later stages of neuropathic pain, exacerbating the pain condition and potentially involving parvalbumin-positive (PV^+) neurons. This study aimed to investigate the effects of voluntary exercise on neuropathic pain-induced anxiety and its relationship with PV^+ neurons, perineuronal nets (PNNs, labeled with Wisteria floribunda agglutinin [WFA]), and microglia in the corticolimbic regions. Male Wistar rats with partial sciatic nerve ligation (PSL) were given access to running wheels either from 3 days (early voluntary exercise [EEx]) or from 4 weeks (late voluntary exercise [LEx]) postoperatively. Nociceptive behaviors were assessed using the von Frey and acetone tests, while anxiety-like behaviors were assessed using the open field and elevated plus maze tests. Brain sections were histologically analyzed using immunohistochemistry and immunofluorescence 8 weeks post-surgery. Both early and late exercise partially restored the paw withdrawal thresholds and the arousal response. PSL-EEx rats did not exhibit anxiety-like behaviors. PSL-LEx rats transiently showed anxiety-like behaviors, but these were eradicated by exercise. PSL altered PV^+ neurons and PNNs in specific corticolimbic subregions. Notably, voluntary exercise restored the densities of PV^+-strong WFA^+ neurons in the basolateral amygdala, PV^+-WFA^-, and PV^+-WFA^+ neurons in the anterior cingulate cortex, and PV^+-WFA^+ neurons in the hippocampal cornu ammonis 1. These changes correlated with reduced anxiety-like behaviors. Exercise modulated PSL-induced microglial activation and interacted differently with these neurons. These findings suggest that voluntary exercise prevents and eliminates chronic pain-induced anxiety through neuronal

Abbreviations: PSL, Partial sciatic nerve ligation; PV, Parvalbumin; GABA, Gamma-Amino Butyric Acid; PNNs, Perineuronal nets; WFA, Wisteria floribunda agglutinin; EEx, Early voluntary exercise; LEx, Late voluntary exercise; Sed, Sedentary; OF, Open field; EPM, Elevated plus maze; PBS, Phosphate-buffered saline; PBS-T, PBS containing 0.25% Triton X-100; DAPI, 4′,6-Diamidino-2-phenylindole; IBA1, Anti-ionized calcium-binding adapter molecule 1; BLC, Basolateral amygdaloid complex; AP, Anterior to posterior; mPFC, Medial prefrontal cortex; ACC, Anterior cingulate cortex; PL, Prelimbic cortex; IL, Infralimbic cortex; CA, Cornu ammonis; DG, Dentate gyrus; sIPSC, spontaneous Inhibitory Postsynaptic Current; MMPs, Matrix metalloproteinases; ADAMTSs, a disintegrin and metalloproteinase with a thrombospondin motif.

* Corresponding author at: Department of Neurorehabilitation and Emotional Science, Graduate School of Biomedical and Health Sciences, Hiroshima University, 1-2-3, Kasumi, Minami-ku, Hiroshima 734-8553, Japan.
E-mail address: urakawas@hiroshima-u.ac.jp (S. Urakawa).

https://doi.org/10.1016/j.ynpai.2025.100181
Received 26 January 2025; Received in revised form 22 February 2025; Accepted 22 February 2025
Available online 27 February 2025

mechanisms other than analgesic effects, potentially involving PV^+ neurons, PNNs, and microglia in the corticolimbic subregions.

1. Introduction

Chronic pain is a global issue imposing significant personal and economic burdens (Cohen et al., 2021) and represents a maladaptive and physiologically disadvantageous condition with complex, multifaceted components. Chronic pain frequently coexists with emotional disorders, such as anxiety, depression, and cognitive dysfunction (Steel et al., 2014). When anxiety disorder accompanies chronic pain, it can worsen pain conditions, leading to poorer quality of life, sleep disturbances, social withdrawal, and more lost workdays compared to chronic pain without anxiety (Velly and Mohit, 2018). Neuropathic pain, which arises directly from an injury or disease affecting the somatosensory system, is a major contributor to chronic pain (Woolf and Mannion, 1999). Our previous study (Dang et al., 2024) demonstrated that rats with partial sciatic nerve ligation (PSL), which mimics clinical neuropathic pain with nociceptive and emotional behavioral disorders, develop anxiety-like behavior in the later stages of the condition. At the brain level, while nociceptive behavior is directly linked to sensory-discriminative pathways (e.g., thalamus and somatosensory cortex), emotional responses are mediated by affective-motivational circuits (e.g., amygdala, medial prefrontal cortex, and hippocampus). Effective treatment of chronic pain requires a multifaceted approach, and successfully addressing its various components is a key strategy.

In addition to pharmacological management, which has encountered challenges in some chronic pain situations, nonpharmacological approaches have been shown to significantly alleviate chronic pain. In particular, physical exercise has demonstrated numerous health benefits, with growing evidence supporting its use as a first-line nonpharmacological treatment for chronic pain disorders (Qaseem et al., 2017). Exercise has been shown to relieve various types of pain, for instance, wide range of pain-relieving effects on mechanical allodynia and heat hyperalgesia (Geneen et al., 2017). Individuals who are physically more active have a lower risk of developing neuropathic pain than those who are less active (Leitzelar and Koltyn, 2021). Furthermore, even in the absence of pain, exercise has been found to significantly benefit psychiatric conditions by reducing depression-like behaviors, alleviating anxiety-like symptoms, improving spatial learning and memory, and promoting resilience to stress in both preclinical and clinical studies (Salmon, 2001). However, the effects of exercise on anxiety disorders induced by chronic pain and their underlying mechanisms have not been fully explored.

It is now recognized that various brain regions involved in chronic pain processing, particularly the limbic system, play pivotal roles in the emotional aspects of pain experiences (Simons et al., 2014), with the inhibitory neuronal network imbalance being a key factor. Parvalbumin-positive (PV^+) neurons, the largest subtype of γ-aminobutyric acid (GABA)-ergic interneurons characterized by their expression of the calcium-binding protein parvalbumin, are crucial in this context (Hu et al., 2014). These neurons orchestrate the synchronized rhythmic activity of the principal neurons through feed-forward inhibition, maintaining a delicate balance between excitatory and inhibitory signals. PV^+ neurons have been implicated in chronic pain (Miyahara et al., 2021) and certain psychiatric disorders (Sgadò et al., 2013). In our previous study (Dang et al., 2024), we observed that anxiety-like behaviors developed in PSL rats were associated with changes in PV^+ neurons within specific corticolimbic subregions. Based on these data, we analyzed the effects of exercise on anxiety-like behavior in chronic pain, focusing on PV^+ neurons in the present study.

The extracellular space contains a complex network of proteins that assemble into dense, net-like structures known as perineuronal nets (PNNs). These PNNs predominantly encase the cell somas and proximal neurites of PV^+ interneurons. PNNs serve as diffusion barriers for ion channels and receptors, scaffolds for binding signaling molecules, and ionic buffers (Fawcett et al., 2019). They regulate cell-to-cell communication and protect neurons from oxidative stress (Morawski et al., 2004), thereby modulating neuronal network functions. Emerging evidence indicates that PNNs are altered in various neurodevelopmental and neurodegenerative disorders associated with changes in brain activity (Testa et al., 2019), suggesting the involvement of PNN cleavage and reorganization in pain-induced emotional disorders and therapeutic exercises. PNNs consist of hyaluronic acid, tenascin-R, glycoproteins, and chondroitin sulfate proteoglycans. Their visualization often employs the lectin Wisteria floribunda agglutinin (WFA), a lectin that binds to N-acetylgalactosamine residues (Fawcett et al., 2019).

Microglia, the resident innate immune cells of the central nervous system, account for 10–15 % of the total neuroglial cells (Nayak et al., 2014). They continuously monitor the brain's microenvironment for harmful signals and protect against both intrinsic and extrinsic insults. In response to neuroinflammatory cytokines, microglia transition to an active state, characterized by phenotypical and morphological changes (Jurga et al., 2020). The activation of spinal microglia following peripheral nerve injury is well documented in the development of hyperalgesia associated with neuropathic pain (Inoue and Tsuda, 2018). Additionally, supraspinal microglia may contribute to both the sensory and affective components of neuropathic pain (Yoshimoto et al., 2023). Although microglia play a protective role under normal physiological conditions, their activation can affect neuronal function, leading to neuronal dysregulation (Kettenmann et al., 2013). The interactions between microglia, PNN structures, and PV^+ neurons as well as the effects of voluntary exercise on these interactions in rats with neuropathic pain, remain unknown.

Therefore, this study aimed to elucidate the effects of voluntary exercise on anxiety-like behavior induced by neuropathic pain and determine whether these effects are associated with alterations in PV^+ neurons, PNN structures, and microglia within the corticolimbic regions.

2. Method

1.1. Animals and neuropathic pain model

Eight-week-old male Wistar rats (purchased from Japan SLC, Shizuoka, Japan) were used in this study. The neuropathic pain model was induced by PSL surgery after a one-week acclimation period, as previously described (Dang et al., 2024; Seltzer et al., 1990). Briefly, under deep anesthesia induced by an intraperitoneal injection of medetomidine (0.15 mg/kg), midazolam (2 mg/kg), and butorphanol (2.5 mg/kg), approximately one-third to one-half of the left sciatic nerve at the midthigh level was tightly ligated with 6–0 silk sutures. The additional experiment was conducted with the right sciatic nerve ligation. Sham surgery was performed following the same procedure except for nerve ligation. Following surgery, all rats received atipamezole (Antisedan®, 0.15 mg/kg) to reverse anesthesia before being returned to their home cages. Lighting (8:00 to 20:00), temperature (22–24 °C), and humidity (70 %–80 %) were controlled throughout the experimental period. The rats were provided food and water ad libitum. This study was approved by the Institutional Animal Care and Use Committee of Hiroshima University (A20-159) and was conducted in accordance with the Hiroshima University Regulations for Animal Experimentation. All experiments were performed in accordance with the National Institutes of Health Guidelines for the Care and Use of Laboratory Animals.

1.2. Voluntary exercise and experimental design

A running wheel (31 cm in diameter) was used for voluntary exercise, placed inside square cages (36 cm in length and 38 cm in height), and connected to a sensor device for counting revolutions (VELO 9; CATEYE, Osaka, Japan). During the night-time (20:00–8:00; active time for experimental animals), rats were individually housed in these running wheel cages for the exercise period, with free access to food and water, mirroring conditions in their home cages. To acclimate to the exercise equipment, all rats were exposed to the running wheel for 3 days before neuropathic pain induction. Our previous study (Dang et al., 2024) found that anxiety-like behaviors emerge in the late phase of PSL rats (starting 4 weeks after surgery). To evaluate the effectiveness of voluntary exercise on this emotional disorder, the intervention was applied to PSL rats during either the early phase (3 days after surgery, early exercise, PSL-EEx group, n = 6) or the late phase (4 weeks after surgery, late exercise, PSL-LEx group, n = 6), with exercise sessions scheduled 5 days per week. The PSL rats that did not exercise (Sedentary, PSL-Sed group, n = 6) and sham-operated rats (n = 6) were housed in standard cages without wheels throughout the experiment. At 8 weeks after surgery, the rat brains were harvested for histological analysis (Fig. 1).

1.3. Assessment of nociceptive behaviors

The von Frey and acetone tests were used to assess the behavioral responses to mechanical and cold stimuli, respectively. Both tests were conducted during the daytime before surgery (pre-surgery), on the 3rd day post-surgery, and weekly thereafter. Rats were individually placed in testing chambers equipped with wire mesh platforms (Ugo Basile SRL, Italy) and allowed to habituate to the testing environment for 30 min. The test sessions were recorded using a camera (PowerShot SX720 HS; Canon, Tokyo, Japan) for subsequent analyses.

1.3.1. Von Frey test

The filaments (Aesthesio® Tactile Sensory Evaluator Kits, USA) were applied manually, perpendicular to the plantar surface of the hind paws, so that the filament bent slightly. Initially, we evaluated mechanical allodynia by identifying the withdrawal threshold using incremental filament forces, as described in our previous study (Dang et al., 2024). Briefly, each filament was applied five times, with the force gradually increasing until a positive response of over 40 % was observed, which was characterized by brisk paw withdrawal, licking, or shaking.

Since uninjured rats exhibited positive responses to a 26 g filament, that force was applied to the surgical paw of all rats to assess hyperalgesia response behaviors. The filament was applied three times at 2-minute intervals. The duration of response (within a 10-second window after pressing the filament to the paw plantar surface) and the response level (scored as 0, no response; 1, brisk withdrawal or flicking of the paw; 2, repeated flicking; 3, repeated flicking and licking of the paw) were recorded.

1.3.2. Acetone test

Following the von Frey test, acetone (50 μl) was gently dropped onto the plantar surface of the surgical paw using a pipette connected to a blunt rubber tube. A brisk paw withdrawal response after dropping was considered a positive response, and the response levels were classified according to a four-point scale: 0, no response; 1, brisk withdrawal or flicking of the paw; 2, repeated flicking of the paw; and 3, repeated flicking of the hind paw and paw licking. The acetone drop was applied five times at 5-minute intervals between each application. The frequency of paw withdrawal was expressed as a percentage: (number of trials accompanied by brisk paw withdrawal) × 100 / (total number of trials). The latency to the paw response was recorded during the 20 s after dropping. The duration of the response was measured from the starting response until it ceased and was recorded up to a maximum duration of 40 s. The response levels were the graded-point averages of five acetone drop trials.

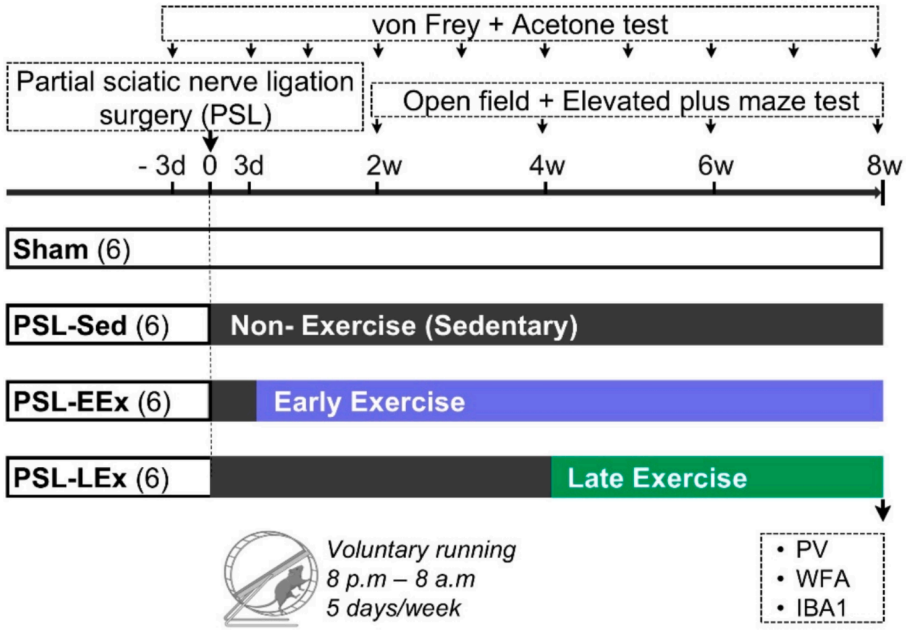

Fig. 1. Experimental design. Eight-week-old male Wistar rats underwent partial sciatic nerve ligation (PSL) surgery to establish a neuropathic pain model. Following surgery, PSL rats were randomly divided into three groups: PSL-Sed (no running wheel access), PSL-EEx (running wheel access starting 3 days post-surgery, early exercise), and PSL-LEx (running wheel access starting 4 weeks post-surgery, late exercise). Nociceptive behaviors were evaluated using von Frey and acetone tests before surgery and weekly thereafter. Anxiety-like behaviors were assessed biweekly using open field and elevated plus maze tests. Eight weeks after surgery, the rats' brains were collected for histological analysis. PSL, partial sciatic nerve ligation; Sed, sedentary; EEx, early exercise; LEx, late exercise; PV, parvalbumin; WFA, Wisteria floribunda agglutinin; IBA1, ionized calcium-binding adapter molecule 1.

1.4. Assessment of anxiety-like behaviors

Anxiety-like behaviors were evaluated using open field (OF) and elevated plus maze (EPM) tests, as described previously (Dang et al., 2024). These assessments were conducted biweekly after surgery during the night-time, with each test day being distinct from the days designated for nociceptive behavior tests. Following acclimatization in the testing room, the rats were given 10 min to freely explore the OF and EPM. Behavioral observations were recorded via video, and the apparatus was sanitized with 70 % ethanol after each trial.

1.4.1. Open field test

The OF apparatus comprised a 90 cm-diameter circular black plastic sheet enclosed by a 70 cm-high wall. The rats were initially placed in the central zone (45 cm in diameter) under 310 lx illumination. Locomotion and time spent in different zones were analyzed using the Animal-Tracker package of the ImageJ software (National Institute of Health, Bethesda, MD, USA), while rearing (rising on the hind limbs) and other activities were manually recorded.

1.4.2. Elevated plus maze test

The EPM apparatus consisted of four arms, each 50 cm long and 10 cm wide, elevated 60 cm above the floor. Two arms were enclosed by 50 cm-high walls (closed arms), while the remaining two arms were open. The illumination levels were set to 325 lx at the ends of the open arms, 21 lx at the ends of the closed arms, and 250 lx at the intersection area. Rats were then placed at the intersection area to begin the test. The analysis focused on the time spent in different arms, frequency of arm entry, and frequency of head dips over the edge upon entering the open arms, with arm entry defined as all four paws crossing into an arm. All the other activities were recorded manually.

Reduced activity in the center zone of the OF and/or open arms of the EPM indicates anxiety-like behavior.

1.5. Tissue preparation

All histological analyses were performed at 8 weeks post-surgery after finishing behavior tests. All rats underwent transcardial perfusion with heparin saline solution and 4 % paraformaldehyde in 0.1 M phosphate buffer following deep pentobarbital anesthesia (100 mg/kg, intraperitoneal). Subsequently, their brains were extracted and preserved in the same fixative for 24 h at 4 °C, after which they were transferred to a 30 % sucrose solution until they sank. The brains were then sliced coronally at a thickness of 30 μm using a freezing microtome (REM-710 + Electro Freeze MC-802C; Yamato Kohki, Saitama, Japan) and were stored in a cryoprotectant solution (glycerol: ethylene glycol: phosphate-buffered saline, 3:3:4) at − 30 °C until further use.

1.6. Immunoperoxidase single staining

For immunoperoxidase staining, we followed the techniques described in our previous study with minor modifications (Dang et al., 2024). Free-floating sections were washed three times in phosphate-buffered saline (PBS), quenched in 2 % hydrogen peroxide (H_2O_2) and 20 % methanol, washed in PBS containing 0.25 % Triton X-100 (PBS-T), and blocked with 3 % normal horse serum for 30 min. After washing in PBS-T, the sections were incubated either with rabbit anti-PV (1:10,000, Sigma, St. Louis, MO, USA) or biotinylated WFA (1:200, B-1355, Vector Laboratories, Burlingame, CA, USA) in 1 % blocking solution for 1 day at room temperature (25 °C) and 1 day at 4 °C. For PV staining, the sections were incubated with a biotinylated anti-rabbit antibody (1:500; Vector Laboratories) on ice for 1 h. After washing in PBS-T, all sections were incubated with an avidin–biotin-peroxidase complex (1:200; ABC-Elite, Vector Laboratories), washed in PBS, and then incubated with 0.025 % diaminobenzidine (DAB, Dojindo Laboratories, Kumamoto, Japan) and 0.03 % H_2O_2. Finally, after dehydration in ethanol and clearing in xylene, the sections were coverslipped with Entellan New (Merck, Darmstadt, Germany).

1.7. Immunofluorescence triple staining

For immunofluorescence staining, sections were rinsed three times in PBS and then incubated simultaneously with rabbit anti-PV antibody (1:5000; Sigma), biotinylated WFA (1:200, B-1355, Vector Laboratories), and mouse anti-ionized calcium-binding adapter molecule 1 (IBA1, for detecting microglia) antibody (1:5000, Merck Millipore, Burlington, MA, USA) in 1 % blocking solution for one day at room temperature (25 °C) and 1 day at 4 °C. After that, the sections were incubated in sequence with Alexa Fluor 555-conjugated goat anti-rabbit IgG (1:500; Cell Signaling Technology, Danvers, MA, USA), Avidin D FITC (1:500, Vector Laboratories), and DyLight™ 405-conjugated goat anti-mouse IgG (1:500; Pierce Biotechnology, Rockford, IL, USA) each for 1 h at room temperature. Finally, the sections were mounted on MAS-coated glass slides using an anti-fade solution (without DAPI; Vector Laboratories). For all staining procedures, negative control sections were processed in the same manner, but without the primary antibody. No reaction products were observed in any of the control samples.

1.8. Microscopic imaging and cell quantification from immunoperoxidase staining

Immunoperoxidase single staining was used to quantify the number of PV^+ and WFA^+ neurons. Images were captured using a light microscope (BX51; Olympus, Tokyo, Japan) equipped with a camera (DP70; Olympus) and a 20 × dry objective lens. These images were analyzed using ImageJ with the Cell Counter package (https://imagej.nih.gov/ij/plugins/cell-counter.html). Within the areas of interest, cells exhibiting PV and WFA immunoreactivity above the background levels were identified as PV^+ and WFA^+ neurons, respectively. Signals from blood vessels, blood cells, or reaction precipitates were excluded from the analysis.

Given that PV + neurons in the amygdala and dorsal hippocampal subregions (Dang et al., 2024) and perineuronal nets (PNNs) in the medial prefrontal cortex (mPFC) (Li et al., 2024; Lee and Lee, 2021) have been associated with anxiety-like behaviors, histological analysis was performed in the following brain regions: the basolateral amygdaloid complex (BLC) of amygdala at anterior-posterior (AP) positions − 2.28, −2.46, and − 2.64 mm; the mPFC — including the prelimbic cortex (PL), infralimbic cortex (IL), and anterior cingulate cortex (ACC)— at AP positions + 3.12, +2.94, and + 2.76 mm; and the dorsal hippocampus, including cornu ammonis (CA) areas 1, 2, and 3, and the dentate gyrus (DG) at AP positions − 2.76, −2.94, and − 3.12 mm from the bregma. Neuronal density estimates (cells/mm^2) were calculated. PV^+ neuron density differed significantly between the left and right hemispheres only in the BLC, with no hemispheric differences observed in the mPFC, dorsal hippocampal subregions, or other cell types. Therefore, cell densities in the mPFC and dorsal hippocampal subregions are presented as averages of both hemispheres.

1.9. Microscopic imaging and cell quantification from immunofluorescence triple staining

To analyze the immunofluorescence staining sections, images (1024 × 1024 pixels, 581.25 × 581.25 μm) were captured using a confocal laser scanning microscope (STELLARIS 5; Leica Microsystems, Wetzlar, Germany) from two or three representative sections for each region. The laser intensity, gain, offset, and pinhole settings were kept constant during the image capture for each region. To quantify PV^+, WFA^+ neurons, and microglia, a 20 × dry objective lens was used to obtain 10 z-stack images with a 2-μm thickness, while a 40 × oil objective lens was used to capture images of microglia bulbous endings within the center of the tissue section.

For cell density and distance analyses, the images were processed using LAS X Office version 1.4.6 (Leica Microsystems). This software allows for simultaneous navigation of positive signals in both merged and single-channel images at the z-stack level or in the overlaid image.

For cell size and intensity analyses, the overlay images of the 10 z-stack images were converted to TIFF format. For microglia bulbous ending intensity analyses, a z-stack image at the midsection was also converted to TIFF. ImageJ was subsequently used to measure the area and intensity of the objects of interest using the freehand selection method on greyscale-converted images. After subtracting the background intensity, the mean intensity of each object was recorded to represent individual objects.

2.9. Statistical analysis

Statistical analyses were conducted using IBM SPSS Statistics (version 19.0; IBM Corp., Armonk, NY, USA). Data are presented as mean ± standard error of the mean (SEM). The Shapiro–Wilk test was used to assess normality, and Levene's test was used to evaluate the homogeneity of variance. For normally distributed data, analyses were performed using an analysis of variance (ANOVA) for multiple comparisons, followed by Tukey's post-hoc test. For non-normal distributions, the Kruskal–Wallis test was performed for multiple comparisons, followed by Dunn's multiple comparisons test. Correlations were evaluated using Spearman's rank correlation coefficient with Bonferroni-adjusted p-values where appropriate. In all cases, p-values were two-tailed, and comparisons were considered statistically significant at $\alpha = 0.05$.

Strategy for classifying WFA intensities.

WFA intensity was classified into weak and strong signal intensity categories. The threshold was set as the mean intensity of the cell population in each brain region of the sham group. Since WFA intensities exhibited a skewed distribution, the geometric means were calculated following logarithmic transformations.

3. Results

3.1. Running parameters and nociceptive behavior

After surgery, both PSL-EEx and PSL-LEx rats initially ran shorter distances but gradually returned to their pre-surgery levels in distance, average velocity, and maximum velocity, all of which remained stable until the end of the experiment (Supplemental Fig. 1).

In the von Frey test, all PSL rats exhibited significantly decreased withdrawal thresholds in the ipsilateral hind paw after surgery, demonstrated by Tukey's tests with a significant interaction between group and time ($F[24, 120] = 6.2$, $p < 0.05$; Fig. 2A). The PSL-Sed rats maintained a low withdrawal threshold throughout the experiment, with a significant difference compared to the sham group ($p < 0.001$). The paw withdrawal threshold of the PSL-EEx rats gradually increased, showing significant differences compared to the PSL-Sed group from 2 to 8 weeks after surgery ($p < 0.05$). The PSL-LEx rats exhibited a significantly higher threshold than that of the PSL-Sed group from 6 to 8 weeks postoperatively ($p < 0.05$). However, the analgesic effect at 8 weeks post-surgery was limited, the thresholds of PSL-EEx rats (16.0 ± 2.2 g) and PSL-LEx rats (12.2 ± 1.3 g) remained significantly lower than that of the sham group (24.2 ± 1.8 g), with p-values of 0.028 and 0.025, respectively. With the 26 g filament application (Fig. 2B), the sham rats demonstrated a weak response to the stimulation (almost score 1), while the PSL-Sed rats exhibited robust responses with significantly higher

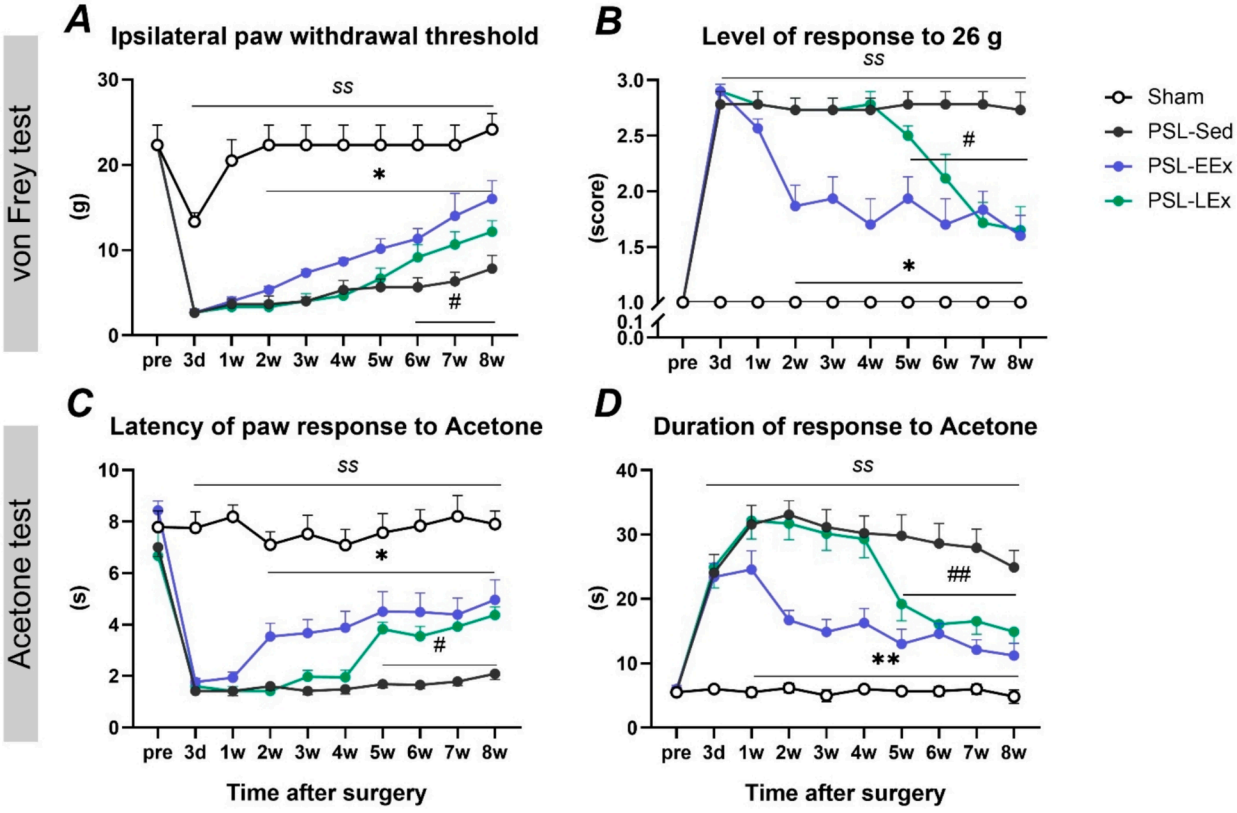

Fig. 2. von Frey and acetone test results. (A) The ipsilateral hind paw withdrawal threshold was detected with incremental force filaments and (B) average level of the response when applying the 26 g filament to the ipsilateral hind paw in the von Frey tests. (C) Latency from the start of dropping acetone onto the ipsilateral hind paw until rats presented the first response and (D) the duration of that response during the acetone tests. Data are presented as mean ± SEM, two-way repeated-measures ANOVA, Tukey's post hoc test, $^{ss}p < 0.001$ (PSL-Sed vs. Sham), $^{*}p < 0.05$ (PSL-EEx vs. PSL-Sed), $^{\#}p < 0.05$ (PSL-LEx vs. PSL-Sed). PSL, partial sciatic nerve ligation; Sed, sedentary; EEx, early exercise; LEx, late exercise; pre, pre-surgery; d, day; w, week.

scores at all time points ($p < 0.001$ vs. sham group) (interaction group × time $F[24, 120] = 5.9$, $p < 0.001$). The differences in response levels between the PSL-EEx group and the PSL-Sed group became statistically significant from 2 to 8 weeks after surgery ($p < 0.05$). The PSL-LEx group demonstrated significantly lower response levels after one week of running (from 5 to 8 weeks postoperatively) than those of the PSL-Sed group ($p < 0.05$). And similarly, 8 weeks after surgery, the mean response level of PSL-EEx rats (1.60 ± 0.18) and PSL-LEx rats (1.65 ± 0.21) remained higher than that of the sham group (1.0 ± 0), with p-values of 0.043 and 0.034, respectively. The response duration parameter followed a similar pattern (Supplemental Fig. 2A).

In the acetone test, PSL-Sed rats exhibited a more significant reduction in withdrawal latency (1–3 s) than that of the sham rats (7–9 s) at the end of the experiment ($p < 0.001$). The interaction between group and time was also significant ($F[24, 120] = 6.8$, $p < 0.05$, Fig. 2C), indicating a low threshold response to cold stimuli. Both EEx and LEx alleviated this condition. The withdrawal latency of the PSL-EEx rats was significantly higher than that of the PSL-Sed rats from 2 to 8 weeks after surgery ($p < 0.05$). Additionally, the withdrawal latency of the PSL-LEx group increased significantly after 1 week of running (from 5 to 8 weeks postoperatively) than those of the PSL-Sed group ($p < 0.05$). And similar to the von Frey test, 8 weeks after surgery, the withdrawal latency of PSL-EEx rats (4.9 ± 0.7 s) and PSL-LEx rats (4.3 ± 0.3 s) remained shorter than that of the sham group (7.9 ± 0.5 s), with p-values of 0.013 and 0.011, respectively. Sham rats exhibited a transient response to the acetone drop, lasting 5–10 s, whereas PSL-Sed rats had a significantly longer response duration of 25–40 s throughout the experiment ($p < 0.001$ vs. sham; Fig. 2D). The interaction between group and time was also significant ($F[24, 120] = 6.1$, $p < 0.05$). This behavior was alleviated after one week of running in both the PSL-EEx group (from 1 to 8 weeks postoperatively, $p < 0.001$ vs. PSL-Sed) and PSL-LEx group (from 5 to 8 weeks postoperatively, $p < 0.001$ vs. PSL-Sed). The response scores to acetone showed a similar pattern (Supplemental Fig. S2B).

These results indicate that voluntary exercise partially restored the paw response threshold to mechanical and cold stimuli and alleviated the arousal response to these stimuli.

3.2. Anxiety-like behavior test results

In the OF test, PSL-Sed rats spent less time in the center zone compared with the sham group starting 4 weeks after surgery, with a significant interaction between group and time ($F[9, 45] = 6.2$, $p < 0.05$; Fig. 3A). In contrast, the PSL-EEx rats did not exhibit this reduction at any time point and maintained the time spent in the center, comparable to that of the sham group. The PSL-LEx rats initially spent similar amounts of time in the center zone as did the PSL-Sed rats 4 weeks after surgery (before starting voluntary exercise). However, the PSL-LEx rats increased their time in the center after two weeks of voluntary exercise (6 weeks after surgery), eventually matching the levels of the sham and PSL-EEx rats ($p < 0.05$ vs. the PSL-Sed group). In the center zone, the rats engaged in walking, running, or rearing activities. The PSL-Sed rats demonstrated a reduction in rearing activity in the center zone compared with the sham group 4 weeks after surgery. Conversely, the PSL-EEx rats maintained activity levels comparable to those of the sham rats, while the PSL-LEx rats recovered their activity to match that of the sham group, with a significant interaction between group and time ($F[9, 45] = 7.3$, $p < 0.05$; Fig. 3B). A similar statistically significant effect was observed 8 weeks after surgery for the center distance traveled and from 6 weeks after surgery for the total number of rearings (Supplemental Table 1). EEx prevented the decline in activity in the center zone, while LEx fully restored the activity levels that had declined in the PSL rats.

In the EPM test, the PSL-Sed rats spent less time in the open arms from 4 weeks after surgery than did the sham group. Meanwhile, the PSL-EEx rats maintained a similar duration in the open arms as the sham group throughout the experiment, with a significant interaction between

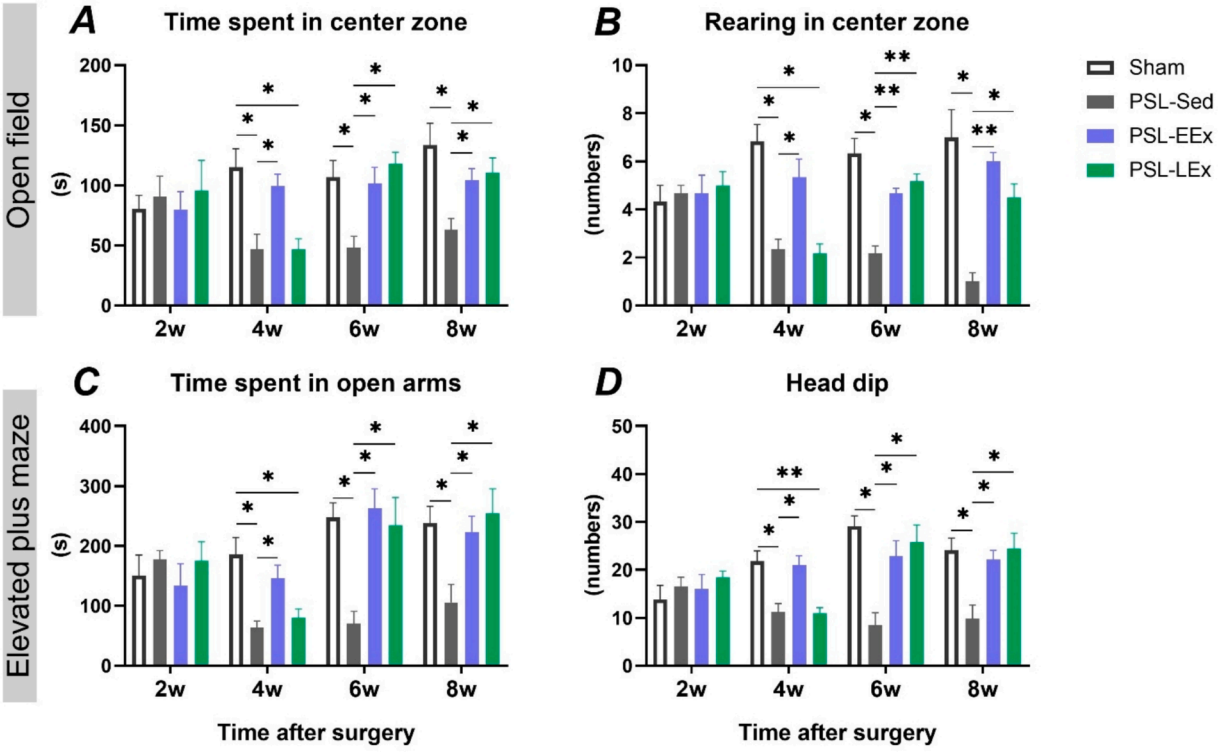

Fig. 3. Open field and elevated plus maze test results. Time spent (A) and number of rearings (B) in the center zone of the open field. Time spent in the open arms (C) and the number of head dip over the edge (D) in the elevated plus maze. Data are presented as mean ± SEM, two-way repeated-measures ANOVA, Tukey's post hoc test, *$p < 0.05$, **$p < 0.001$. PSL, partial sciatic nerve ligation; Sed, sedentary; EEx, early exercise; LEx, late exercise.

group and time ($F[9, 45] = 4.8$, $p < 0.05$; Fig. 3C). After a decrease in the open arm duration in the PSL-LEx group 4 weeks after surgery, this parameter significantly recovered to match the levels of the sham group at 6 and 8 weeks post-surgery ($p < 0.05$ vs. PSL-Sed group). The number of entries into the open arms followed the same pattern as the time spent in the open arms (Supplemental Table 1). Exploratory activity in the open arms, measured by head-dipping activity, indicated that EEx prevented the decline in exploratory activities, and LEx alleviated the decline that had already occurred in PSL rats, bringing their activity levels in line with those of the sham group. This finding was supported by a significant interaction between group and time ($F[9, 45] = 5.3$, $p < 0.05$; Fig. 3D).

These results indicate that voluntary exercise positively influences anxiety-like behavior in PSL rats. EEx prevented the emergence of these behaviors, and LEx completely restored these emotional stability once these disorders had already developed in PSL rats.

3.3. Alterations of PV^+ and WFA^+ neurons in amygdala subregion

In the BLC, the single staining method revealed a significant difference between the groups in the density of PV^+ neurons (Fig. 4A), but not in WFA^+ neurons (Fig. 4B). In the BLC, the PV^+ neuron density was reduced in PSL-Sed rats, while both voluntary exercise groups restored this density to levels comparable to those of sham rats, as indicated by one-way ANOVA ($F[3, 20] = 19.2$, $p < 0.001$). The PV^+ neuron density was comparable between the left and right BLC in the sham, PSL-Sed, and PSL-EEx groups. However, it was higher in the right BLC than in the left BLC in the PSL-LEx group (Fig. 4A), with a significant interaction between group and time ($F[3, 15] = 10.9$, $p < 0.05$, two-way ANOVA).

Using triple staining (Fig. 4C), we classified the PV^+ and/or WFA^+ neurons into three categories: PV^+ neurons without PNNs (PV^+-WFA^-), PV^+ neurons with PNNs (PV^+-WFA^+), and other WFA^+ neurons (PV^--WFA^+). The density of PV^+-WFA^+ neurons was reduced in PSL-Sed rats, whereas in both voluntary exercise groups, it was comparable to that of

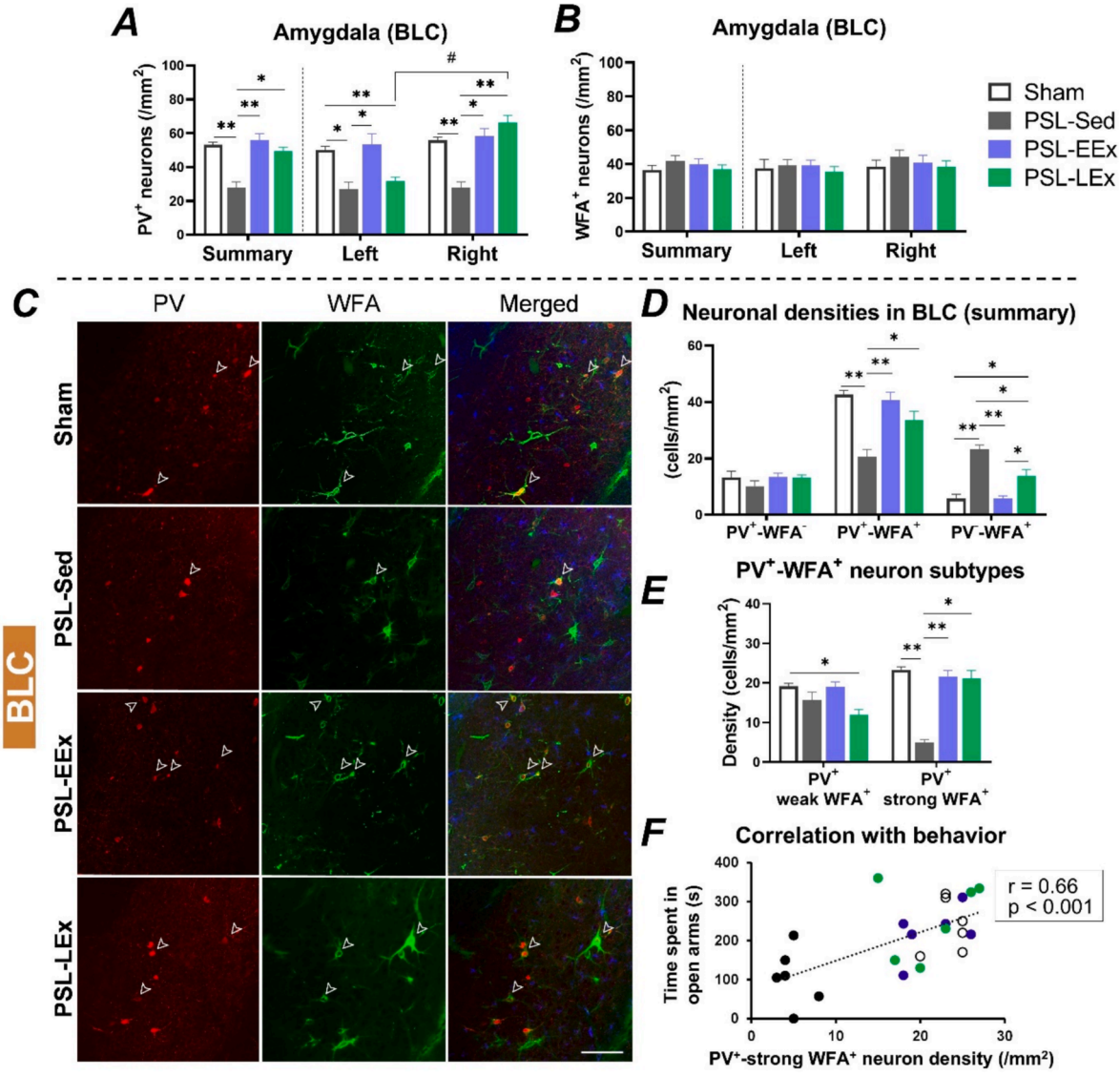

Fig. 4. PV^+ and WFA^+ neurons in the BLC. (A) Density of PV^+ neurons and (B) WFA^+ neurons in the basolateral amygdala complex (BLC) region (shown for each side and summarized). (C) Representative immunofluorescence triple-staining images for PV, WFA, and IBA1 in the right BLC; unfilled arrowheads indicate PV^+-strong WFA^+ neurons (scale bar = 100 μm). (D) Density of neurons. (E) Density of PV^+-WFA^+ neuron subtypes, where PV^+-WFA^+ neurons are divided into PV^+-weak WFA^+ and PV^+-strong WFA^+ neurons using a threshold of 11.4 arbitrary units, based on the mean WFA intensity of the sham group (after log-transformation). (F) Correlation of PV^+-strong WFA^+ neuron density with anxiety-like behavior parameters. Data are presented as mean ± SEM. One-way or two-way ANOVA, Tukey's post hoc test, *$p < 0.05$, **$p < 0.001$ (between groups), $^{\#}p < 0.05$ (left vs right). Spearman's rank correlation significance is indicated at $p < 0.05$. PV, parvalbumin; WFA, Wisteria floribunda agglutinin; PSL, partial sciatic nerve ligation; Sed, sedentary; EEx, early exercise; LEx, late exercise.

the sham group, as indicated by Tukey's tests after one-way ANOVA ($F[3, 20] = 15.3$, $p < 0.001$) (Fig. 4D). This finding mirrored the changes observed in anxiety-like behavior. Additionally, the neuronal somata size and the intensity of PV and WFA expression were examined (Supplemental Fig. 2A, B, C). In sham rats, PV^+-WFA^+ neurons were larger and exhibited stronger PV intensity signals than PV^+-WFA^- neurons. While the somatic size of PV^+-WFA^+ neurons did not differ between the groups, the intensities of both PV and WFA were affected by PSL surgery and exercise interventions.

We further classified PV^+-WFA^+ neurons into PV^+-weak WFA^+ and PV^+-strong WFA^+ neurons based on WFA intensity, using a threshold of 11.4 a.u. as the log-transformed mean intensity of the sham group population (neurons with WFA intensity < 11.4 a.u. were classified as weak WFA, and neurons with WFA intensity ≥ 11.4 a.u. were classified as strong WFA). Notably, changes in PV^+-WFA^+ neurons induced by PSL surgery or exercise were primarily observed in PV^+-strong WFA^+ neurons (Fig. 4E), and their density significantly correlated with the time spent in the open arms of the EPM test (Fig. 4F).

Differences in PV^+ neuron density between the left and right hemispheres were observed in the BLC of the PSL-LEx group with left surgical hind paw, but not in the mPFC or dorsal hippocampus. To explore the potential lateralization effect associated with the side of neuropathy, we conducted an additional experiment using rats with right sciatic nerve ligation exposed to late exercise (right-ligation PSL-LEx, Supplemental Fig. 4). The results revealed that the effects of late exercise on nociceptive and anxiety-like behaviors were similar between the left- and right-ligation PSL rats. In the right-ligation PSL rats, PV^+ neuron density was comparable between both BLC sides, matching the levels observed in the sham group.

These results suggest that PSL-induced alterations in PV^+ neurons in the BLC were restored by voluntary exercise, primarily affecting PV^+-strong WFA^+ neurons, and were associated with anxiety-like behaviors.

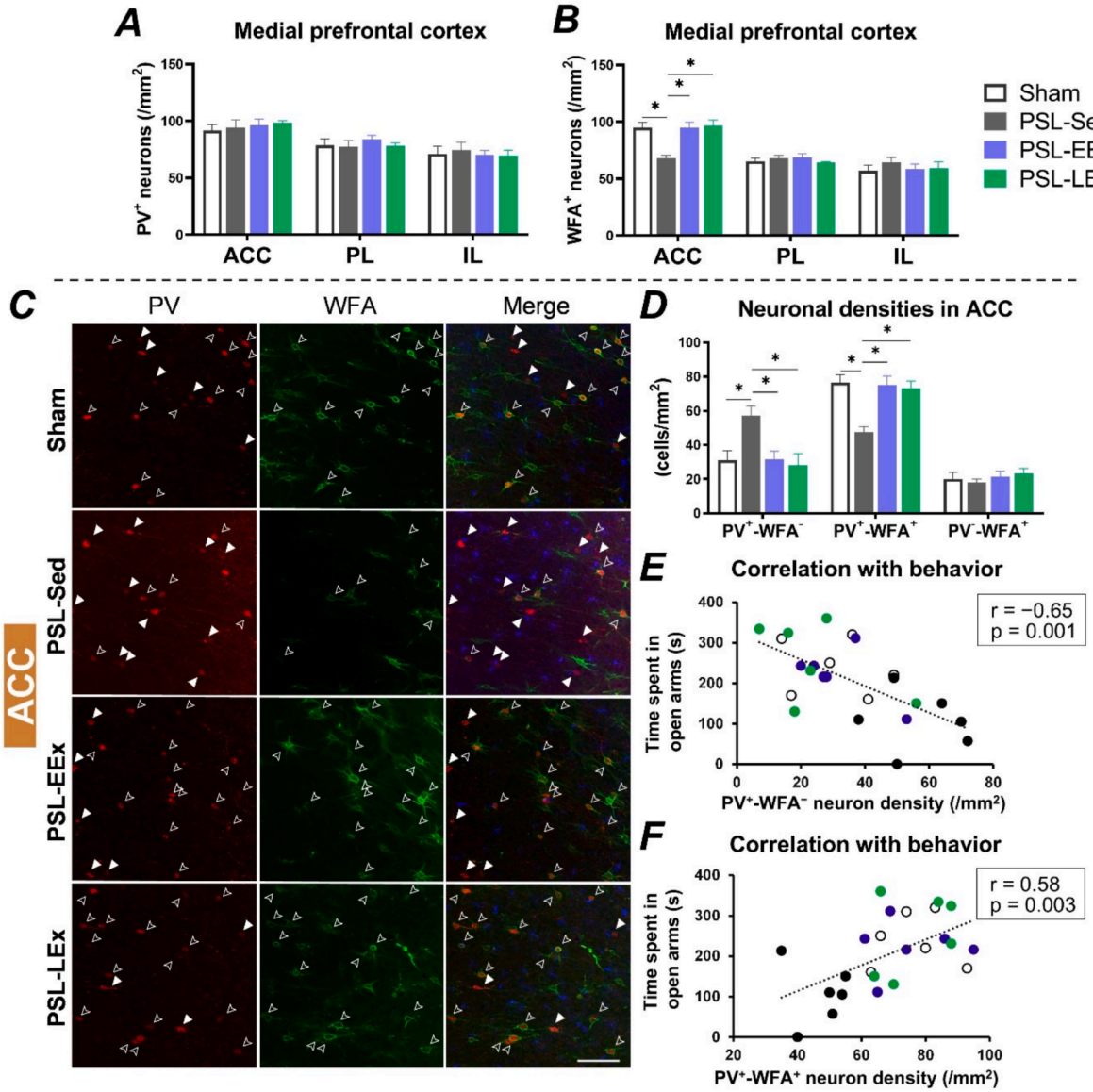

Fig. 5. PV^+ and WFA^+ neurons in the ACC. (A) Density of PV^+ neurons and (B) WFA^+ neurons in the medial prefrontal cortex subregions. (C) Representative images of immunofluorescence triple staining for PV, WFA, and IBA1 in the right ACC; unfilled arrowheads indicate PV^+-WFA^+ neurons, filled arrowheads indicate PV^+-WFA^- neurons (scale bar = 100 μm). (D) Density of neurons in the ACC. (E) Correlation of PV^+-WFA^- neuron density, (F) PV^+-WFA^+ neuron density and anxiety-like behavior parameter. Data are presented as mean ± SEM. One-way ANOVA, Tukey's post hoc test, *$p < 0.05$. Spearman's rank correlation significance is indicated at $p < 0.05$. PV, parvalbumin; WFA, Wisteria floribunda agglutinin; ACC, anterior cingulate cortex; PL, prelimbic cortex; IL, infralimbic cortex; PSL, partial sciatic nerve ligation; Sed, sedentary; EEx, early exercise; LEx, late exercise.

Additionally, the side of the surgical hind paw affected PV^+ neuron density in the BLC of PSL-LEx rats, with the right BLC exerting a strong effect on anxiety-like behavior, regardless of the side of neuropathy.

3.4. Alterations of PV^+ and WFA^+ neurons in medial prefrontal cortex subregions

The single staining method revealed a significant difference in the density of WFA^+ neurons in the ACC between groups, while no differences were observed in the PV^+ neurons across any subregion of the mPFC (PL and IL) (Fig. 5A, B). WFA^+ neuron density was reduced in the PSL-Sed group, whereas in both voluntary exercise groups, this parameter was restored to levels comparable to those of the sham group, as indicated by Tukey's tests after one-way ANOVA ($F[3, 20] = 9.3$, $p < 0.001$).

Triple staining demonstrated that WFA^+ neuronal alterations in the ACC were significant in PV^+-WFA^+ neurons (Fig. 5C, D). The density of PV^+-WFA^+ neurons decreased in the PSL-Sed rats, whereas in both voluntary exercise groups, this parameter was comparable to that of the sham group, as indicated Tukey's tests after by one-way ANOVA ($F[3, 20] = 9.8$, $p < 0.001$). In contrast, the density of PV^+-WFA^- neurons increased in the PSL-Sed rats, whereas in both voluntary exercise groups, this parameter was similar to that in the sham group. Notably, the densities of PV^+-WFA^- and PV^+-WFA^+ neurons in the ACC were significantly correlated with the time spent in the open arms during the EPM test (Fig. 5E, F).

The reduced WFA intensity of PV^+-WFA^+ neurons induced by PSL surgery was restored with early voluntary exercise (Supplemental Fig. 5C). However, no specific subtype of PV^+-WFA^+ neurons, classified based on WFA intensity (same method as in the BLC region with a

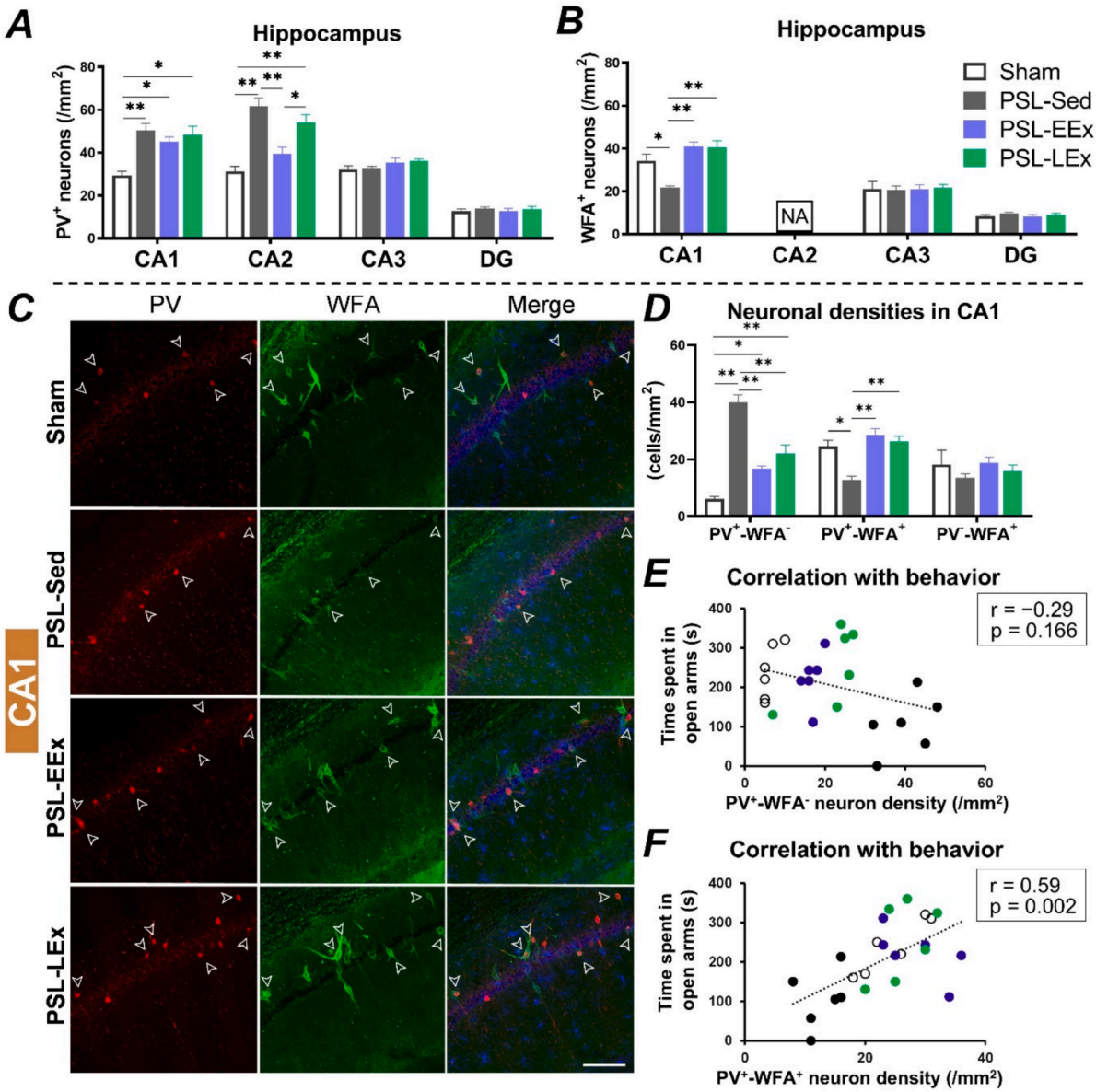

Fig. 6. PV^+ and WFA^+ neurons in the dorsal CA1. (A) Density of PV^+ neurons and (B) WFA^+ neurons in the dorsal hippocampal subregions. (C) Representative images of immunofluorescence triple staining for PV, WFA, and IBA1 in the right dorsal CA1; unfilled arrowheads indicate PV^+-WFA^+ neurons (scale bar = 100 μm). (D) Density of neurons in the dorsal CA1 subregion. (E) Correlation of PV^+-WFA^- neuron density, (F) PV^+-WFA^+ neuron density and anxiety-like behavior parameter. Data are presented as mean ± SEM. One-way ANOVA, Tukey's post hoc test, *$p < 0.05$ and **$p < 0.001$. Spearman's rank correlation significance is indicated at $p < 0.05$. PV, parvalbumin; WFA, Wisteria floribunda agglutinin; CA1–3, cornu ammonis areas 1–3; DG, dentate gyrus; NA, non-application; PSL, partial sciatic nerve ligation; Sed, sedentary; EEx, early exercise; LEx, late exercise.

threshold of 16.1 a.u.), was associated with anxiety-like behavior parameters.

These results indicate that PSL-induced WFA alterations in the ACC, leading to changes in PV^+-WFA^- and PV^+-WFA^+ neurons, were influenced by voluntary exercise and related to anxiety-like behaviors.

3.5. Alterations of PV^+ and WFA^+ neurons in dorsal hippocampal subregions

In the dorsal hippocampus, single staining revealed the effects of PSL surgery and exercise on PV^+ and WFA^+ neurons in the CA1 (Fig. 6A, B), as well as PV^+ neurons in the CA2 (Supplemental Fig. 7B, C). In CA2, WFA staining was intense, encasing all the neuron bodies in the stratum pyramidale; therefore, the density of WFA^+ neurons was not assessed. In CA1, the PV^+ neuron density increased in all rats that underwent PSL surgery, regardless of exercise, as indicated by Tukey's tests after one-way ANOVA ($F[3, 20] = 10.1$, $p < 0.001$), whereas the WFA^+ neuron density was reduced in PSL-Sed rats but restored with both early and late exercise, as indicated by Tukey's tests after one-way ANOVA ($F[3, 20] = 13.4$, $p < 0.001$). In CA2, the increased PV^+ neuron density observed in PSL-Sed rats was suppressed by early exercise but not by late exercise, as indicated by Tukey's tests after one-way ANOVA ($F[3, 20] = 17.4$, $p < 0.001$).

In the CA1 region, triple staining revealed that the effects of PSL surgery and/or voluntary exercise were significant for both PV^+-WFA^- and PV^+-WFA^+ neurons (Fig. 6D). The density of PV^+-WFA^- neurons was increased in the PSL-Sed rats; although this parameter was altered in both voluntary exercise groups, it did not reach the levels observed in the sham group. The density of PV^+-WFA^+ neurons decreased in the PSL-Sed group, but in both voluntary exercise groups, PV^+-WFA^+ neuron densities were comparable to those in the sham group, as indicated by Tukey's tests after one-way ANOVA ($F[3, 20] = 12.9$, $p < 0.001$). Analysis of the correlation between these neuron densities and anxiety-like behavior parameters revealed that the density of PV^+-WFA^+ neurons significantly correlated with the time spent in the open arms of the EPM test (Fig. 6E, F).

The PV intensity and WFA intensity were altered by PSL surgery and exercise intervention (Supplemental Fig. 6B, C). However, the correlation between PV^+-WFA^+ neuron density and anxiety-like behavior parameters was not solely attributable to any of these neuronal subtypes (classified based on WFA intensity using the same method as in the BLC region with a WFA threshold of 13.2 a.u.).

In the CA2 region, the densities of PV^+-WFA^- and PV^+-WFA^+ neurons varied between the groups (Supplemental Fig. 7) but were not related to anxiety-like behavior parameters.

These results demonstrate that in the dorsal hippocampus, PSL-induced PV^+-WFA^+ and PV^+-WFA^- neuron alterations were influenced by voluntary exercise, with PV^+-WFA^+ neurons in the CA1 region being related to anxiety-like behaviors.

3.6. Relationships of neuronal alterations among different corticolimbic subregions

Given that PV^+-WFA^+ neurons in distinct corticolimbic subregions were altered by PSL surgery and/or exercise intervention, multiple correlation analyses were conducted to investigate the relationship between these regional alterations and their association with anxiety-like behaviors. Significant correlations were observed between the densities of PV^+-strong WFA^+ neurons in the BLC, PV^+-WFA^+ neurons in the ACC, and PV^+-WFA^+ neurons in the CA1 (Table 1).

3.7. Microglia and their interaction with PV^+ and WFA^+ neurons in corticolimbic subregions

Although the density of microglia in the BLC did not differ between the groups (Supplemental Fig. 3D), their morphology was altered by PSL surgery and exercise intervention. The percentage of amoeboid-shaped microglia increased in the PSL-Sed group but was significantly reduced in both voluntary exercise groups compared to the PSL-Sed group, as indicated by one-way Tukey's tests after ($F[3, 20] = 28.9$, $p < 0.001$) (Fig. 7D). Microglia in the PSL-Sed group exhibited larger bodies with stronger signals and shorter processes than did both voluntary exercise groups. Additionally, voluntary exercise reversed these changes in body intensity and altered process length (Supplemental Fig. 3E, F, G). To assess microglia-neuron interactions, we measured the distance between neurons and microglia as well as the intensity of microglial bulbous endings ($IBA1^+$ signal) around neurons. In the PSL-Sed rats, microglia were in closer contact with PV^+-WFA^-, PV^+-strong WFA^+, and PV^--WFA^+ neurons than were microglia in both exercise groups. In contrast, the distances between microglia and PV^+-strong WFA^+ and PV^--WFA^+ neurons in both exercise groups were similar to those observed in the sham group (Fig. 7E). The intensity of microglial bulbous endings around PV^+-WFA^-, PV^+-strong WFA^+, and PV^--WFA^+ neurons was higher in the PSL-Sed group than in the sham group. In contrast, the intensities in the exercise groups were comparable to those in the sham group (Fig. 7F).

In the ACC, microglia density did not differ between the groups (Supplemental Fig. 5D). The PSL-Sed rats exhibited more amoeboid-shaped microglia and fewer ramified-shaped microglia than did the sham rats (Fig. 7G). In the PSL-EEx rats, the percentage of amoeboid-shaped microglia decreased to a level similar to that of the sham rats, while in the PSL-LEx rats, the percentage of ramified-shaped microglia increased to a level comparable to that of the sham rats. Microglia in the PSL-Sed group also exhibited larger bodies and shorter processes than did those in the sham group, while these characteristics were modified by voluntary exercise (Supplemental Fig. 5E, F, G). In the PSL-Sed rats, microglia were in closer contact with PV^+-WFA^- neurons, whereas in both voluntary exercise groups, the distance between PV^+-WFA^- neurons and the nearest microglia was similar to that in sham rats (Fig. 7H). Microglial bulbous endings around PV^+-WFA^- neurons were more prominent in the PSL-Sed rats than in the sham group. In contrast, both voluntary exercise groups demonstrated reduced levels of microglial bulbous endings to the same level as sham rats (Fig. 7I).

In the CA1, while the morphology of microglia did not differ between the groups (Fig. 7J), notable differences were observed in the distribution of microglia across distinct layers of CA1. Specifically, there was an increased density in the pyramidal layer of PSL-Sed rats, which was restored by voluntary exercise (Fig. 7L). In the PSL-Sed rats, microglia were in closer contact with PV^+-WFA^- neurons, whereas in both voluntary exercise groups, the distance between PV^+-WFA^- neurons and the nearest microglia was similar to that in sham rats (Fig. 7K).

In the CA2, microglial changes followed the same pattern as that in the CA1; however, contact with PV^+ neurons was not specific to PV^+-WFA^- or PV^+-WFA^+ neurons (Supplemental Fig. 7).

These results indicate that PSL led to microglia activation, and the interactions of microglia with PV^+ and WFA^+ neurons were altered

Table 1
Correlation matrix of neuron densities in limbic subregions and anxiety-like behavior parameter.

	1	2	3
1. BLC (PV^+-strong WFA^+ neuron density)			
2. ACC (PV^+-WFA^+ neuron density)	0.85 (0.006)		
3. CA1 (PV^+-WFA^+ neuron density)	0.57 (0.024)	0.64 (0.006)	
4. Time spent in open arms	0.66 (0.006)	0.59 (0.018)	0.59 (0.012)

Data represents Spearman's rank correlation coefficient (Bonferroni adjusted p-value).
Significant at the α level of 0.05.

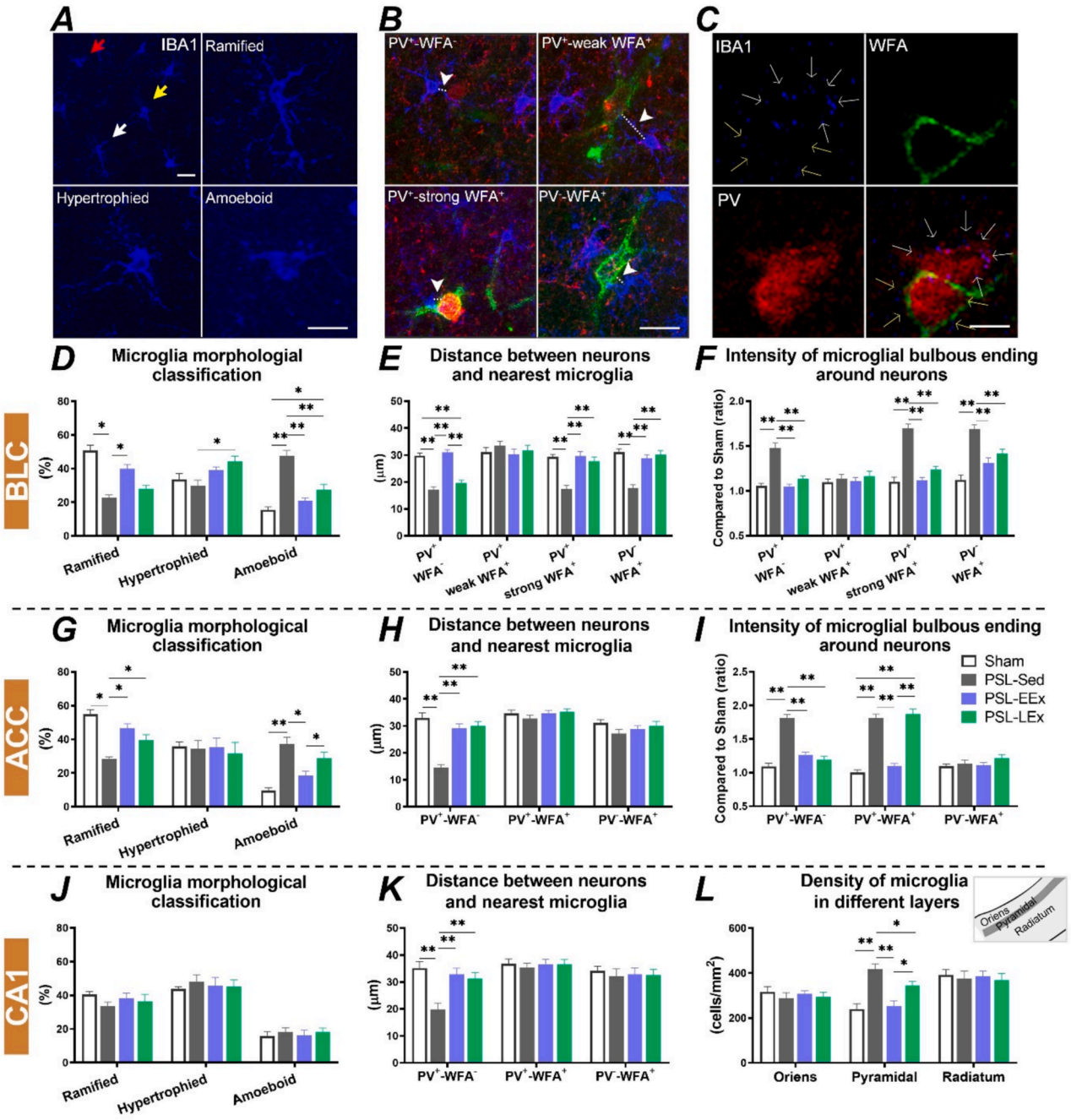

Fig. 7. Microglia and their interaction with PV$^+$ and WFA$^+$ neurons in the BLC, ACC, and dorsal CA1. (A) Representative images of microglia (labeled by IBA1), morphologically classified as ramified (white arrows at top left, magnified at top right), hypertrophied (yellow arrows at top left, magnified at bottom left), and amoeboid (red arrows at top left, magnified at bottom right) (scale bar = 20 μm). (B) Representative images showing the distance (white dotted lines with white arrowheads) between different neurons and the nearest microglia (scale bar = 20 μm). (C) Representative images illustrating microglial bulbous endings around PV$^+$-WFA$^-$ neurons (white arrows) and around PV$^+$-WFA$^+$ neurons (yellow arrows) (scale bar = 10 μm). Microglial morphological classification, distance between different neurons and the nearest microglia, and the intensity of microglial bulbous endings around neurons (presented as a ratio relative to the sham group, N = 30/type/group) in the BLC (D, E, F) and ACC (G, H, I). (J) Microglial morphological classification, (K) distance between different neurons and the nearest microglia, and (L) densities of microglia in different layers of dorsal CA1. Data are presented as mean ± SEM. One-way ANOVA, Tukey's post hoc test, *$p < 0.05$ and **$p < 0.001$. PV, parvalbumin; WFA, Wisteria floribunda agglutinin; IBA1, ionized calcium-binding adapter molecule 1; BLC, basolateral amygdala complex; ACC, anterior cingulate cortex; CA1, cornu ammonis area 1; PSL, partial sciatic nerve ligation; Sed, sedentary; EEx, early exercise; LEx, late exercise. (For interpretation of the references to colour in this figure legend, the reader is referred to the web version of this article.)

differently in distinct corticolimbic subregions, which were modulated by voluntary exercise.

4. Discussion

In this study, we found that voluntary exercise had a beneficial impact on both nociceptive pain and neuropathic pain-induced anxiety-like behaviors in rats subjected to PSL. While nociceptive behaviors were partially improved by voluntary exercise, neuropathic pain-induced anxiety-like behavior was prevented by early voluntary exercise and completely eliminated by late voluntary exercise. Voluntary exercise restored the density of various neuron types: PV$^+$-strong WFA$^+$ neurons

in the BLC, PV^+-WFA^- and PV^+-WFA^+ neurons in the ACC, and PV^+-WFA^+ neurons in the CA1 region, all of which correlated with anxiety-like behaviors. PSL-induced microglia activation interacted differently with these neurons and was modulated by voluntary exercise. Late exercise had different effects on PV^+ neuron density in the left and right BLC.

The primary goal of this study was to examine the effects of voluntary exercise on anxiety-like behaviors induced by neuropathic pain. We introduced voluntary exercise in PSL rats at two different time points: soon after PSL surgery (before the onset of anxiety-like behavior, EEx) and at a later stage (after anxiety-like behavior had already been established, LEx). Our findings revealed that PSL-EEx rats maintained normal exploratory activity, similar to the sham group, whereas PSL-LEx rats showed recovery in exploratory activity, eventually reaching control levels. These results suggest that voluntary exercise can prevent anxiety-like behaviors through early intervention and can eliminate them even in the chronic phase of neuropathic pain. Although the benefits of exercise in reducing pain intensity in patients with chronic pain are well documented (Geneen et al., 2017), its impact on the emotional dimensions of chronic pain remains underexplored. Pain is a complex and subjective experience involving both physical sensations and emotional responses. In our nociceptive tests, we observed that alongside a partial recovery in nociceptive thresholds, arousal responses to mechanical and cold stimuli were also alleviated by voluntary exercise, indicating an improvement in both allodynia and emotional disorders. Clinically, differentiating between the physical and emotional effects of chronic pain is challenging because of the shared neurobiological features of pain and neuropsychiatric diseases (Bushnell et al., 2013; Hooten, 2016). However, our study found that voluntary exercise not only eliminated pain-induced anxiety but also partially recovered allodynia in PSL rats. Furthermore, exercise training has been shown to effectively reduce depression and anxiety in patients with musculoskeletal pain (Amiri, 2023), enhance the quality of life in patients with chronic neuropathic pain (Zhang et al., 2021), and benefit animals with neuropathic pain (Cheng et al., 2022; Klein et al., 2021). Therefore, the positive effects of voluntary exercise on anxiety-like behaviors may contribute to its analgesic effects and improvement of chronic neuropathic pain.

The second goal of this study was to investigate the effects of voluntary exercise on neurobiological changes associated with emotional alterations in PSL rats. We corroborated our earlier findings (Dang et al., 2024) that PSL induces changes in PV^+ neurons in the amygdala and dorsal hippocampus. Additionally, we observed concurrent changes in WFA^+ neurons in both regions and the ACC. Voluntary exercise restored WFA^+ neurons in the ACC and CA1, while its effects on PV^+ neurons were observed in the BLC and CA2. Notably, PV^+-WFA^+ neurons in the BLC, ACC, and CA1 correlated with anxiety-like behaviors and were similarly restored through voluntary exercise. These results suggest the potential role of PV^+-WFA^+ neurons in distinct corticolimbic subregions in mediating the reversed effects of voluntary exercise on neuropathic pain-induced anxiety. In the BLC, reductions in PV^+-WFA^+ neurons have been linked to emotional disorders induced by early-life traumatic stress (Guadagno et al., 2020; Santiago et al., 2018) and juvenile-adolescent social isolation (Vazquez-Sanroman et al., 2021). Additionally, PV^+ neurons are involved in the effects of multiple anxiogenic drugs (Hale et al., 2010), and PV^+-WFA^+ neurons are influenced by an enriched environment that promotes increased physical activity and reduces anxiety-like behaviors (Urakawa et al., 2013; Vazquez-Sanroman et al., 2021). In the hippocampal CA1 region, alterations in PV^+-WFA^+ neurons have been linked to the anxiety-like behavior index in inescapable foot shock rats (Fan et al., 2024). Notably, the initial apparent loss of PNNs and PV^+ neurons in stressed adult animals can recover over several weeks following certain interventions (Koskinen et al., 2020; Riga et al., 2017). Swimming exercise has been shown to activate PV^+ neurons, resulting in anxiolytic-like effects (Selakovic et al., 2017), while running has been found to affect PV expression and increase the density of PV^+ neurons (Gomes da Silva et al., 2010). In the mPFC, mice exhibiting anxiety-like behavior showed a reduction in the density of PV^+-WFA^+ neurons, along with decreased mRNA and protein levels of aggrecan (a core component of PNNs). Additionally, digestion of PNNs using Chondroitinase ABC led to the emergence of anxiety-like behavior (Li et al., 2024). The densities of PV^+-WFA^+ neurons in the mPFC subregion correlate with both the time spent and distance traveled in the center of an OF, which are indicators of basal anxiety-like behavior in adult mice (Lee and Lee, 2021). Additionally, changes in PNNs have been associated with the development of chronic pain (Mascio et al., 2022). Moreover, the anxiolytic effects of fluoxetine, a selective serotonin-reuptake inhibitor, have been reported to involve PV^+-WFA^+ neurons in the BLC and CA1 of rats (Chan et al., 2024) and PNNs in the mPFC of stressed mice (Li et al., 2024). Notably, regular exercise such as voluntary wheel running has been shown to have an effect comparable to that of fluoxetine in alleviating anxiety-like behaviors in stressed animals (Lapmanee et al., 2013). Therefore, the reversal effects of voluntary exercise on chronic pain-induced anxiety may involve PV^+-WFA^+ neurons across different brain regions.

Notably, PV^+-WFA^+ neurons in the BLC were involved in the alleviating effects of voluntary exercise on chronic pain-induced anxiety, predominantly through PV^+-strong WFA^+ neurons. This suggests that a specific PV^+ neuron subtype plays a key role in these effects and is functionally mediated by specific PNNs. We found that PV^+ neurons surrounded by PNNs were larger and exhibited greater PV expression than those without PNNs, which is consistent with our previous findings regarding PV^+ neuron size (Dang et al., 2024). PNNs function as a physical barrier that protects neurons from reactive oxygen species, modulates synaptic transmission and neuronal activity, and maintains the stable function of decorated neurons. Additionally, parvalbumin expression, measured by immunofluorescence intensity, has been shown to correlate with GABA production (Donato et al., 2013; Spijker et al., 2020) and is often considered a reflection of PV^+ neuron activity (Favuzzi et al., 2017; Hijazi et al., 2020). Therefore, the stronger signal of PV expression in PV^+-WFA^+ neurons compared to PV^+-WFA^- neurons in our study suggests that PV^+ neurons with PNNs are more active. Essentially, the level of PNN intensity could influence how effectively the PV^+ neurons perform their functions.

Consequently, alterations in PV^+-WFA^+ neurons may contribute to changes in the activity of principal neurons in certain brain regions. In the BLC of the PSL-Sed rats, we observed a decrease in the density of PV^+-WFA^+ neurons, while the overall density of WFA^+ neurons remained unchanged. Additionally, in the amygdala, PNNs were found to surround both inhibitory and excitatory neurons (Morikawa et al., 2017), suggesting that the increase in PV^--WFA^+ neurons may be partially associated with excitatory neurons. Furthermore, WFA^+ excitatory neurons are particularly susceptible to stimulus activation (Morikawa et al., 2017). In the BLC of rats exhibiting emotional disorders induced by early-life trauma, WFA intensity decreased in parallel with a reduction in axosomatic synapses between PV^+-to-principal pyramidal-like neurons and PV^+-to-PV^+ neurons (Santiago et al., 2018). Therefore, the reduction in PV^+-WFA^+ neurons, particularly PV^+-strong WFA^+ neurons, in the BLC is likely to contribute to the overall decrease in the inhibitory drive onto principal neurons, resulting in increased firing variability among these neurons. In the hippocampus, reduced spontaneous inhibitory postsynaptic current (sIPSC) frequency in pyramidal neurons in adult stress rats is associated with decreased PV^+ neuron activity (Sagi et al., 2020). Robust theta-frequency power in the mPFC has been observed in rats exhibiting anxiety induced by sparse nerve injury (Sang et al., 2018). Notably, the density of PV^+-strong WFA^- neurons in the BLC correlated with the density of PV^+-WFA^+ neurons in the ACC and CA1 and with anxiety-like behavior, suggesting that the amygdala-mPFC-hippocampus circuit regulates neuropathic pain-induced anxiety, with these effects mediated by voluntary exercise. Activated neurons projecting from the CA1 to the BLC have been reported in mice with neuropathic pain, and voluntary exercise suppresses

these hyperactivated hippocampal projection neurons (Minami et al., 2023). Theta-frequency synchronization between the mPFC and hippocampus increases in rats exhibiting anxiety induced by spare nerve injury (Sang et al., 2018). The BLC excitatory projections to the mPFC play an important role in controlling stress behavior, pain, and other emotional disorders (Delli Pizzi et al., 2017; Sangha et al., 2020). However, further studies are required to clarify the involvement and the detailed pathways of this circuit in neuropathic pain-induced anxiety.

We found that microglia were activated and interacted differently with PV^+ and WFA^+ neurons in distinct brain regions of PSL-Sed rats, and these effects were reversed by voluntary exercise. Under normal conditions, microglia survey their environments with highly ramified processes, monitoring synaptic activity and sampling microenvironments. In pathological conditions, they rapidly adopt reactive shapes (Jurga et al., 2020). PSL increased the number of amoeboid-shaped microglia in the BLC and ACC. Additionally, microglia density was higher in the pyramidal neuron layer of the dorsal hippocampal CA1 and CA2, suggesting that PSL activates microglia in these corticolimbic regions. Peripheral nerve injury activates microglia in the brain regions associated with sensory pain transmission (Miyamoto et al., 2017; Taylor et al., 2017). Hyperactivated microglia can cause damage or dysfunction in PNNs and PV neurons in different brain regions. Under normal conditions, microglia secrete matrix metalloproteinases (MMPs) and a disintegrin and metalloproteinases with a thrombospondin motif (ADAMTSs), which cleave the structural components of PNNs to enable dynamic synapse remodeling and changes in neuronal plasticity (Chen et al., 2023; Crapser et al., 2021). However, in states of neuroinflammation due to chronic pain (Sun et al., 2023), upregulation of MMP activity from hyperactivated microglia can result in the abnormal cleavage of PNNs. This observation may elucidate the reduction of PNNs observed in the ACC and dorsal CA1 regions of PSL-Sed rats, where microglia are in closer proximity to and exhibit increased surveillance of PV^+-WFA^- and PV^+-weak WFA^+ neurons. In contrast, the relationship between hyperactivated microglia and damage to or dysfunction of PNNs and PV^+ neurons in the BLC appears to be more complex, with microglia interacting with PV^+-WFA^-, PV^+-strong WFA^+, and PV^--WFA^+ neurons in PSL-Sed rats. Around the PV^+ neurons, MMP upregulation can aberrantly cleave PNNs, thereby exposing PV^+ neurons to toxins. Owing to the high energy demand of PV^+ neurons (Hu et al., 2014), they are particularly susceptible to dysfunction under inflammatory or oxidative conditions. Additionally, microglia are involved in the phagocytic engulfment and elimination of excitatory synapses onto PV^+-WFA^- neurons, resulting in abnormal activity within these neurons. Around PV^--WFA^+ neurons, microglia can selectively prune inhibitory synapses onto projection neurons (Favuzzi et al., 2021). This microglial elimination enhances neural circuit connectivity and activity (Liu et al., 2021). Thus, microglia may contribute to inhibitory dysfunction. Notably, the hyperactivation of microglia and alterations in PV^+ and WFA^+ neurons were mitigated following voluntary exercise, highlighting the significant role of microglia in PV^+ and WFA^+ neuron alterations and their impact on PSL-induced anxiety.

LEx primarily facilitated the recovery of PV^+ neurons in the right BLC of rats with left hind paw PSL. Although LEx had similar effects on nociceptive and anxiety-like behaviors in both the left and right lesioned sides, the restoration of PV + neurons occurred exclusively in the right BLC, indicating a side-specific recovery mechanism. This suggests that PV^+ neurons in the right BLC play a major role in the eradication of pain-induced anxiety by LEx and that the side of the surgical paw can influence this lateralization. Functional differences between the left and right amygdala are influenced by the state of neuropathic pain and its emotional effects. In a rat model of neuropathy, neuronal activity was higher in the left amygdala 2 and 6 days after nerve injury than that in the right amygdala. However, activity in the right amygdala became dominant starting from 2 weeks after surgery, regardless of the injured side (Gonçalves and Dickenson, 2012). The right amygdala is more involved than the left amygdala in producing negative emotions in some chronic pain conditions (Baker and Kim, 2004). Human studies have found that an enlarged right amygdala is associated with social anxiety disorders (Suor et al., 2020), while increased activity in the left anterior brain regions correlates with greater pain catastrophizing (Jensen et al., 2015). Thus, the beneficial effects of voluntary exercise on anxiety-like behavior in the later stages of neuropathic pain may be linked to the increased involvement of the right amygdala. Although we observed that the side of the surgical paw can affect this lateralization, and some studies have reported varying severity of pain-associated emotional disorders depending on the injured side (Leite-Almeida et al., 2012), further research is required to clarify the precise mechanisms underlying these lateralization effects of voluntary exercise on neuropathic pain-induced anxiety.

Our study has certain limitations. First, to minimize the influence of nociceptive behavior tests on anxiety-like behavior assessments, we used only chemical cold stimuli but not heat stimuli for thermal tests, even though nociceptive behavior responses can differ based on the type of stimulus. Second, histological analysis was conducted only after the voluntary exercise intervention. Additional histological analyses during the intervention could offer more insight into the changing dynamics of PV^+ neurons and PNNs and how they relate to the effects of voluntary exercise on pain-induced anxiety. Third, although WFA staining captures most of the molecular components of PNNs, it does not recognize all of them (Matthews et al., 2002). Employing additional histological analyses with other PNN markers, such as aggrecan antibodies, could provide a more comprehensive understanding of PNN structures in the corticolimbic regions of PSL rats. Finally, we analyzed only the dorsal hippocampus subregions, even though the dorsal and ventral hippocampus may serve different functions due to their distinct fiber connections (Trompoukis and Papatheodoropoulos).

5. Conclusion

Voluntary exercise prevented and eradicated pain-induced anxiety-like behaviors in PSL rats, contributing to its analgesic effects. PSL induces changes in PV^+ neurons, PNNs, and activated microglia in specific corticolimbic subregions. Notably, the density of PV^+-strong WFA^+ neurons in the BLC, PV^+-WFA^- and PV^+-WFA^+ neurons in the ACC, and PV^+-WFA^+ neurons in the dorsal CA1 region were restored by voluntary exercise, interacting differently with microglia and correlating with anxiety-like behaviors. Late-stage exercise predominantly affected the PV^+ neurons in the right amygdala. These findings provide new insights into the therapeutic effects of voluntary exercise on anxiety induced by chronic neuropathic pain.

CRediT authorship contribution statement

Thu Nguyen Dang: Writing – review & editing, Writing – original draft, Methodology, Investigation, Formal analysis, Data curation, Conceptualization. **Cuong Nguyen Van:** Writing – review & editing, Visualization. **Ryosuke Ochi:** Writing – review & editing, Methodology. **Hiroki Kuwamura:** Visualization. **Tomoyuki Kurose:** Writing – review & editing, Methodology. **Yoki Nakamura:** Writing – review & editing, Conceptualization. **Kazue Hisaoka-Nakashima:** Writing – review & editing, Conceptualization. **Norimitsu Morioka:** Writing – review & editing, Supervision, Conceptualization. **Hisao Nishijo:** Writing – review & editing, Methodology. **Naoto Fujita:** Writing – review & editing, Methodology. **Susumu Urakawa:** Writing – review & editing, Writing – original draft, Supervision, Project administration, Methodology, Investigation, Funding acquisition, Formal analysis, Conceptualization.

Funding

This work was supported by a Grant-in-Aid for Scientific Research from the Japanese Ministry of Education, Culture, Sports, Science, and Technology (23 K10503; SU), and research funds from Hiroshima

University. The funders had no role in study design, the collection, analysis, and interpretation of data, and the decision to submit the article for publication.

Declaration of competing interest

The authors declare that they have no known competing financial interests or personal relationships that could have appeared to influence the work reported in this paper.

Acknowledgments

A part of this work was carried out at the Analysis Center of Life Science, Natural Science Center for Basic Research and Development, Hiroshima University.

Appendix A. Supplementary data

Supplementary data to this article can be found online at https://doi.org/10.1016/j.ynpai.2025.100181.

Data availability

Data will be made available on request.

References

Amiri, S., 2023. Exercise training and depression and anxiety in musculoskeletal pain patients: a meta-analysis of randomized control trials. Neuropsychiatr. 37 (2), 88–100. https://doi.org/10.1007/s40211-022-00431-2.

Baker, K.B., Kim, J.J., 2004. Amygdalar lateralization in fear conditioning: evidence for greater involvement of the right amygdala. Behav. Neurosci. 118 (1), 15–23. https://doi.org/10.1037/0735-7044.118.1.15.

Bushnell, M.C., Ceko, M., Low, L.A., 2013. Cognitive and emotional control of pain and its disruption in chronic pain. Nat. Rev. Neurosci. 14 (7), 502–511. https://doi.org/10.1038/nrn3516.

Chan, D., Baker, K.D., Richardson, R., 2024. The impact of chronic fluoxetine treatment in adolescence or adulthood on context fear memory and perineuronal nets. Dev. Psychobiol. 66 (5), e22501. https://doi.org/10.1002/dev.22501.

Chen, J., Wang, T., Zhou, Y., Hong, Y., Zhang, S., Zhou, Z., Jiang, A., Liu, D., 2023. Microglia trigger the structural plasticity of GABAergic neurons in the hippocampal CA1 region of a lipopolysaccharide-induced neuroinflammation model. Exp. Neurol. 370, 114565. https://doi.org/10.1016/j.expneurol.2023.114565.

Cheng, X., Yu, Z., Hu, W., Chen, J., Chen, W., Wang, L., Li, X., Zhang, W., Chen, J., Zou, X., Chen, W., Wan, Y., 2022. Voluntary exercise ameliorates neuropathic pain by suppressing calcitonin gene-related peptide and ionized calcium-binding adapter molecule 1 overexpression in the lumbar dorsal horns in response to injury to the cervical spinal cord. Exp. Neurol. 354, 114105. https://doi.org/10.1016/j.expneurol.2022.114105.

Cohen, S.P., Vase, L., Hooten, W.M., 2021. Chronic pain: an update on burden, best practices, and new advances. Lancet. 397 (10289), 2082–2097. https://doi.org/10.1016/s0140-6736(21)00393-7.

Crapser, J.D., Arreola, M.A., Tsourmas, K.I., Green, K.N., 2021. Microglia as hackers of the matrix: sculpting synapses and the extracellular space. Cell. Mol. Immunol. 18 (11), 2472–2488. https://doi.org/10.1038/s41423-021-00751-3.

Dang, T.N., Tien, S.N., Ochi, R., Le Trung, D., Nishio, K., Kuwamura, H., Kurose, T., Fujita, N., Nishijo, H., Nakamura, Y., Hisaoka-Nakashima, K., Morioka, N., Urakawa, S., 2024. Enhanced anxiety-like behavior induced by chronic neuropathic pain and related parvalbumin-positive neurons in male rats. Behav. Brain Res. 459, 114786. https://doi.org/10.1016/j.bbr.2023.114786.

Delli Pizzi, S., Chiacchiaretta, P., Mantini, D., Bubbico, G., Ferretti, A., Edden, R.A., Di Giulio, C., Onofrj, M., Bonanni, L., 2017. Functional and neurochemical interactions within the amygdala-medial prefrontal cortex circuit and their relevance to emotional processing. Brain Struct. Funct. 222 (3), 1267–1279. https://doi.org/10.1007/s00429-016-1276-z.

Donato, F., Rompani, S.B., Caroni, P., 2013. Parvalbumin-expressing basket-cell network plasticity induced by experience regulates adult learning. Nature. 504 (7479), 272–276. https://doi.org/10.1038/nature12866.

Fan, Z., Gong, X., Xu, H., Qu, Y., Li, B., Li, L., Yan, Y., Wu, L., Yan, C., 2024. Hippocampal parvalbumin and perineuronal nets: Possible involvement in anxiety-like behavior in rats. Hippocampus. 34 (3), 156–165. https://doi.org/10.1002/hipo.23595.

Favuzzi, E., Huang, S., Saldi, G.A., Binan, L., Ibrahim, L.A., Fernández-Otero, M., Cao, Y., Zeine, A., Sefah, A., Zheng, K., Xu, Q., Khlestova, E., Farhi, S.L., Bonneau, R., Datta, S.R., Stevens, B., Fishell, G., 2021. GABA-receptive microglia selectively sculpt developing inhibitory circuits. Cell. 184 (15), 4048–4063.e32. https://doi.org/10.1016/j.cell.2021.06.018.

Favuzzi, E., Marques-Smith, A., Deogracias, R., Winterflood, C.M., Sánchez-Aguilera, A., Mantoan, L., Maeso, P., Fernandes, C., Ewers, H., Rico, B., 2017. Activity-Dependent Gating of Parvalbumin Interneuron Function by the Perineuronal Net Protein Brevican. Neuron. 95 (3), 639–655.e610. https://doi.org/10.1016/j.neuron.2017.06.028.

Fawcett, J.W., Oohashi, T., Pizzorusso, T., 2019. The roles of perineuronal nets and the perinodal extracellular matrix in neuronal function. Nat. Rev. Neurosci. 20 (8), 451–465. https://doi.org/10.1038/s41583-019-0196-3.

Geneen, L.J., Moore, R.A., Clarke, C., Martin, D., Colvin, L.A., Smith, B.H., 2017. Physical activity and exercise for chronic pain in adults: an overview of Cochrane Reviews. Cochrane Database Syst. Rev. 4 (4), CD011279. https://doi.org/10.1002/14651858.CD011279.pub3.

Gomes da Silva, S., Doná, F., da Silva Fernandes, M.J., Scorza, F.A., Cavalheiro, E.A., Arida, R.M., 2010. Physical exercise during the adolescent period of life increases hippocampal parvalbumin expression. Brain Dev. 32 (2), 137–142. https://doi.org/10.1016/j.braindev.2008.12.012.

Gonçalves, L., Dickenson, A.H., 2012. Asymmetric time-dependent activation of right central amygdala neurones in rats with peripheral neuropathy and pregabalin modulation. Eur. J. Neurosci. 36 (9), 3204–3213. https://doi.org/10.1111/j.1460-9568.2012.08235.x.

Guadagno, A., Verlezza, S., Long, H., Wong, T.P., Walker, C.D., 2020. It Is All in the Right Amygdala: Increased Synaptic Plasticity and Perineuronal Nets in Male, But Not Female, Juvenile Rat Pups after Exposure to Early-Life Stress. J. Neurosci. 40 (43), 8276–8291. https://doi.org/10.1523/jneurosci.1029-20.2020.

Hale, M.W., Johnson, P.L., Westerman, A.M., Abrams, J.K., Shekhar, A., Lowry, C.A., 2010. Multiple anxiogenic drugs recruit a parvalbumin-containing subpopulation of GABAergic interneurons in the basolateral amygdala. Prog. Neuropsychopharmacol. Biol. Psychiatry. 34 (7), 1285–1293. https://doi.org/10.1016/j.pnpbp.2010.07.012.

Hijazi, S., Heistek, T.S., Scheltens, P., Neumann, U., Shimshek, D.R., Mansvelder, H.D., Smit, A.B., van Kesteren, R.E., 2020. Early restoration of parvalbumin interneuron activity prevents memory loss and network hyperexcitability in a mouse model of Alzheimer's disease. Mol. Psychiatry. 25 (12), 3380–3398. https://doi.org/10.1038/s41380-019-0483-4.

Hooten, W.M., 2016. Chronic Pain and Mental Health Disorders: Shared Neural Mechanisms, Epidemiology, and Treatment. Mayo Clin. Proc. 91 (7), 955–970. https://doi.org/10.1016/j.mayocp.2016.04.029.

Hu, H., Gan, J., Jonas, P., 2014. Interneurons. Fast-spiking, parvalbumin^{+} GABAergic interneurons: from cellular design to microcircuit function. Science. 345 (6196), 1255263. https://doi.org/10.1126/science.1255263.

Inoue, K., Tsuda, M., 2018. Microglia in neuropathic pain: cellular and molecular mechanisms and therapeutic potential. Nat. Rev. Neurosci. 19 (3), 138–152. https://doi.org/10.1038/nrn.2018.2.

Jensen, M.P., Gianas, A., Sherlin, L.H., Howe, J.D., 2015. Pain Catastrophizing and EEG-α Asymmetry. Clin. J. Pain. 31 (10), 852–858. https://doi.org/10.1097/ajp.0000000000000182.

Jurga, A.M., Paleczna, M., Kuter, K.Z., 2020. Overview of General and Discriminating Markers of Differential Microglia Phenotypes. Front. Cell. Neurosci. 14, 198. https://doi.org/10.3389/fncel.2020.00198.

Kettenmann, H., Kirchhoff, F., Verkhratsky, A., 2013. Microglia: new roles for the synaptic stripper. Neuron. 77 (1), 10–18. https://doi.org/10.1016/j.neuron.2012.12.023.

Klein, D., Yuan, X., Weiß, E.M., Martini, R., 2021. Physical exercise mitigates neuropathic changes in an animal model for Charcot-Marie-Tooth disease 1X. Exp. Neurol. 343, 113786. https://doi.org/10.1016/j.expneurol.2021.113786.

Koskinen, M.K., van Mourik, Y., Smit, A.B., Riga, D., Spijker, S., 2020. From stress to depression: development of extracellular matrix-dependent cognitive impairment following social stress. Sci. Rep. 10 (1), 17308. https://doi.org/10.1038/s41598-020-73173-2.

Lapmanee, S., Charoenphandhu, J., Charoenphandhu, N., 2013. Beneficial effects of fluoxetine, reboxetine, venlafaxine, and voluntary running exercise in stressed male rats with anxiety- and depression-like behaviors. Behav. Brain Res. 250, 316–325. https://doi.org/10.1016/j.bbr.2013.05.018.

Lee, J., Lee, K., 2021. Parvalbumin-expressing GABAergic interneurons and perineuronal nets in the prelimbic and orbitofrontal cortices in association with basal anxiety-like behaviors in adult mice. Behav. Brain Res. 398, 112915. https://doi.org/10.1016/j.bbr.2020.112915.

Leite-Almeida, H., Cerqueira, J.J., Wei, H., Ribeiro-Costa, N., Anjos-Martins, H., Sousa, N., Pertovaara, A., Almeida, A., 2012. Differential effects of left/right neuropathy on rats' anxiety and cognitive behavior. Pain. 153 (11), 2218–2225. https://doi.org/10.1016/j.pain.2012.07.007.

Leitzelar, B.N., Koltyn, K.F., 2021. Exercise and Neuropathic Pain: A General Overview of Preclinical and Clinical Research. Sports Med. Open. 7 (1), 21. https://doi.org/10.1186/s40798-021-00307-9.

Li, X., Ren, D., Luo, B., Liu, Z., Li, N., Zhou, T., Fei, E., 2024. Perineuronal Nets Alterations Contribute to Stress-Induced Anxiety-Like Behavior. Mol. Neurobiol. 61 (1), 411–422. https://doi.org/10.1007/s12035-023-03596-1.

Liu, Y.J., Spangenberg, E.E., Tang, B., Holmes, T.C., Green, K.N., Xu, X., 2021. Microglia Elimination Increases Neural Circuit Connectivity and Activity in Adult Mouse Cortex. J. Neurosci. 41 (6), 1274–1287. https://doi.org/10.1523/jneurosci.2140-20.2020.

Mascio, G., Notartomaso, S., Martinello, K., Liberatore, F., Bucci, D., Imbriglio, T., Cannella, M., Antenucci, N., Scarselli, P., Lattanzi, R., Bruno, V., Nicoletti, F., Fucile, S., Battaglia, G., 2022. A Progressive Build-up of Perineuronal Nets in the Somatosensory Cortex Is Associated with the Development of Chronic Pain in Mice. J. Neurosci. 42 (14), 3037–3048. https://doi.org/10.1523/jneurosci.1714-21.2022.

Matthews, R.T., Kelly, G.M., Zerillo, C.A., Gray, G., Tiemeyer, M., Hockfield, S., 2002. Aggrecan glycoforms contribute to the molecular heterogeneity of perineuronal nets.

J. Neurosci. 22 (17), 7536–7547. https://doi.org/10.1523/jneurosci.22-17-07536.2002.
Minami, K., Kami, K., Nishimura, Y., Kawanishi, M., Imashiro, K., Kami, T., Habata, S., Senba, E., Umemoto, Y., Tajima, F., 2023. Voluntary running-induced activation of ventral hippocampal GABAergic interneurons contributes to exercise-induced hypoalgesia in neuropathic pain model mice. Sci. Rep. 13 (1), 2645. https://doi.org/10.1038/s41598-023-29849-6.
Miyahara, K., Nishimaru, H., Matsumoto, J., Setogawa, T., Taguchi, T., Ono, T., Nishijo, H., 2021. Involvement of Parvalbumin-Positive Neurons in the Development of Hyperalgesia in a Mouse Model of Fibromyalgia. Front. Pain Res. 2, 627860. https://doi.org/10.3389/fpain.2021.627860.
Miyamoto, K., Kume, K., Ohsawa, M., 2017. Role of microglia in mechanical allodynia in the anterior cingulate cortex. J. Pharmacol. Sci. 134 (3), 158–165. https://doi.org/10.1016/j.jphs.2017.05.010.
Morawski, M., Brückner, M.K., Riederer, P., Brückner, G., Arendt, T., 2004. Perineuronal nets potentially protect against oxidative stress. Exp. Neurol. 188 (2), 309–315. https://doi.org/10.1016/j.expneurol.2004.04.017.
Morikawa, S., Ikegaya, Y., Narita, M., Tamura, H., 2017. Activation of perineuronal net-expressing excitatory neurons during associative memory encoding and retrieval. Sci. Rep. 7, 46024. https://doi.org/10.1038/srep46024.
Nayak, D., Roth, T.L., McGavern, D.B., 2014. Microglia development and function. Annu. Rev. Immunol. 32, 367–402. https://doi.org/10.1146/annurev-immunol-032713-120240.
Qaseem, A., Wilt, T.J., McLean, R.M., Forciea, M.A., Denberg, T.D., Barry, M.J., Boyd, C., Chow, R.D., Fitterman, N., Harris, R.P., Humphrey, L.L., Vijan, S., 2017. Noninvasive Treatments for Acute, Subacute, and Chronic Low Back Pain: A Clinical Practice Guideline From the American College of Physicians. Ann. Intern. Med. 166 (7), 514–530. https://doi.org/10.7326/m16-2367.
Riga, D., Kramvis, I., Koskinen, M.K., van Bokhoven, P., van der Harst, J.E., Heistek, T.S., Jaap Timmerman, A., van Nierop, P., van der Schors, R.C., Pieneman, A.W., de Weger, A., van Mourik, Y., Schoffelmeer, A.N.M., Mansvelder, H.D., Meredith, R.M., Hoogendijk, W.J.G., Smit, A.B., Spijker, S., 2017. Hippocampal extracellular matrix alterations contribute to cognitive impairment associated with a chronic depressive-like state in rats. Sci. Transl. Med. 9 (421). https://doi.org/10.1126/scitranslmed.aai8753.
Sagi, Y., Medrihan, L., George, K., Barney, M., McCabe, K.A., Greengard, P., 2020. Emergence of 5-HT5A signaling in parvalbumin neurons mediates delayed antidepressant action. Mol. Psychiatry. 25 (6), 1191–1201. https://doi.org/10.1038/s41380-019-0379-3.
Salmon, P., 2001. Effects of physical exercise on anxiety, depression, and sensitivity to stress: a unifying theory. Clin. Psychol. Rev. 21 (1), 33–61. https://doi.org/10.1016/s0272-7358(99)00032-x.
Sang, K., Bao, C., Xin, Y., Hu, S., Gao, X., Wang, Y., Bodner, M., Zhou, Y.D., Dong, X.W., 2018. Plastic change of prefrontal cortex mediates anxiety-like behaviors associated with chronic pain in neuropathic rats. Mol. Pain. 14, 1744806918783931. https://doi.org/10.1177/1744806918783931.
Sangha, S., Diehl, M.M., Bergstrom, H.C., Drew, M.R., 2020. Know safety, no fear. Neurosci. Biobehav. Rev. 108, 218–230. https://doi.org/10.1016/j.neubiorev.2019.11.006.
Santiago, A.N., Lim, K.Y., Opendak, M., Sullivan, R.M., Aoki, C., 2018. Early life trauma increases threat response of peri-weaning rats, reduction of axo-somatic synapses formed by parvalbumin cells and perineuronal net in the basolateral nucleus of amygdala. J. Comp. Neurol. 526 (16), 2647–2664. https://doi.org/10.1002/cne.24522.
Selakovic, D., Joksimovic, J., Zaletel, I., Puskas, N., Matovic, M., Rosic, G., 2017. The opposite effects of nandrolone decanoate and exercise on anxiety levels in rats may involve alterations in hippocampal parvalbumin-positive interneurons. PloS One. 12 (12), e0189595. https://doi.org/10.1371/journal.pone.0189595.
Seltzer, Z., Dubner, R., Shir, Y., 1990. A novel behavioral model of neuropathic pain disorders produced in rats by partial sciatic nerve injury. Pain. 43 (2), 205–218. https://doi.org/10.1016/0304-3959(90)91074-s.
Sgadò, P., Genovesi, S., Kalinovsky, A., Zunino, G., Macchi, F., Allegra, M., Murenu, E., Provenzano, G., Tripathi, P.P., Casarosa, S., Joyner, A.L., Bozzi, Y., 2013. Loss of GABAergic neurons in the hippocampus and cerebral cortex of Engrailed-2 null mutant mice: implications for autism spectrum disorders. Exp. Neurol. 247, 496–505. https://doi.org/10.1016/j.expneurol.2013.01.021.
Simons, L.E., Elman, I., Borsook, D., 2014. Psychological processing in chronic pain: A neural systems approach. Neurosci. Biobehav. Rev. 39, 61–78. https://doi.org/10.1016/j.neubiorev.2013.12.006.
Spijker, S., Koskinen, M.K., Riga, D., 2020. Incubation of depression: ECM assembly and parvalbumin interneurons after stress. Neurosci. Biobehav. Rev. 118, 65–79. https://doi.org/10.1016/j.neubiorev.2020.07.015.
Steel, Z., Marnane, C., Iranpour, C., Chey, T., Jackson, J.W., Patel, V., Silove, D., 2014. The global prevalence of common mental disorders: a systematic review and meta-analysis 1980-2013. Int. J. Epidemiol 43 (2), 476–493. https://doi.org/10.1093/ije/dyu038.
Sun, C., Deng, J., Ma, Y., Meng, F., Cui, X., Li, M., Li, J., Li, J., Yin, P., Kong, L., Zhang, L., Tang, P., 2023. The dual role of microglia in neuropathic pain after spinal cord injury: Detrimental and protective effects. Exp. Neurol. 370, 114570. https://doi.org/10.1016/j.expneurol.2023.114570.
Suor, J.H., Jimmy, J., Monk, C.S., Phan, K.L., Burkhouse, K.L., 2020. Parsing differences in amygdala volume among individuals with and without social and generalized anxiety disorders across the lifespan. J. Psychiatr. Res. 128, 83–89. https://doi.org/10.1016/j.jpsychires.2020.05.027.
Taylor, A.M., Mehrabani, S., Liu, S., Taylor, A.J., Cahill, C.M., 2017. Topography of microglial activation in sensory- and affect-related brain regions in chronic pain. J. Neurosci. Res. 95 (6), 1330–1335. https://doi.org/10.1002/jnr.23883.
Testa, D., Prochiantz, A., Di Nardo, A.A., 2019. Perineuronal nets in brain physiology and disease. Semin. Cell Dev. Biol. 89, 125–135. https://doi.org/10.1016/j.semcdb.2018.09.011.
Trompoukis, G., Papatheodoropoulos, C., 2020. Dorsal-Ventral Differences in Modulation of Synaptic Transmission in the Hippocampus. Front. Synaptic Neurosci. 12, 24. https://doi.org/10.3389/fnsyn.2020.00024.
Urakawa, S., Takamoto, K., Hori, E., Sakai, N., Ono, T., Nishijo, H., 2013. Rearing in enriched environment increases parvalbumin-positive small neurons in the amygdala and decreases anxiety-like behavior of male rats. BMC Neurosci. 14, 13. https://doi.org/10.1186/1471-2202-14-13.
Vazquez-Sanroman, D.B., Arlington Wilson, G., Bardo, M.T., 2021. Effects of Social Isolation on Perineuronal Nets in the Amygdala Following a Reward Omission Task in Female Rats. Mol. Neurobiol. 58 (1), 348–361. https://doi.org/10.1007/s12035-020-02125-8.
Velly, A.M., Mohit, S., 2018. Epidemiology of pain and relation to psychiatric disorders. Prog. Neuropsychopharmacol. Biol. Psychiatry. 87, 159–167. https://doi.org/10.1016/j.pnpbp.2017.05.012.
Woolf, C.J., Mannion, R.J., 1999. Neuropathic pain: aetiology, symptoms, mechanisms, and management. Lancet. 353 (9168), 1959–1964. https://doi.org/10.1016/s0140-6736(99)01307-0.
Yoshimoto, N., Nakamura, Y., Hisaoka-Nakashima, K., Morioka, N., 2023. Mitochondrial dysfunction and type I interferon signaling induce anxiodepressive-like behaviors in mice with neuropathic pain. Exp. Neurol. 367, 114470. https://doi.org/10.1016/j.expneurol.2023.114470.
Zhang, Y.H., Hu, H.Y., Xiong, Y.C., Peng, C., Hu, L., Kong, Y.Z., Wang, Y.L., Guo, J.B., Bi, S., Li, T.S., Ao, L.J., Wang, C.H., Bai, Y.L., Fang, L., Ma, C., Liao, L.R., Liu, H., Zhu, Y., Zhang, Z.J., Liu, C.L., Fang, G.E., Wang, X.Q., 2021. Exercise for Neuropathic Pain: A Systematic Review and Expert Consensus. Front. Med. 8, 756940. https://doi.org/10.3389/fmed.2021.756940.